2016

Use of Clearview Gel Dosimeter for Quality Assurance and Testing of Stereotactic Radiosurgery

Erik Joseph-Leonard Courter
Wright State University

USE OF CLEARVIEW GEL DOSIMETER FOR QUALITY ASSURANCE AND TESTING OF STEREOTACTIC RADIOSURGERY

A thesis submitted in partial fulfillment

of the requirements for the degree of

Master of Science

By

Erik Joseph-Leonard Courter

B.S. in Medical Physics, Oakland University, 2014

2016

Wright State University

WRIGHT STATE UNIVERSITY

GRADUATE SCHOOL

April 19, 2016

I HEARBY RECOMMEND THAT THE THESIS PREPARED UNDER MY SUPERVISION BY **Erik Joseph-Leonard Courter**ENTITLED **Use of ClearView Gel Dosimeter for Quality Assurance and Testing of Stereotactic Radiosurgery** BE ACCEPTED IN PARTIAL FULFILLMENT OF THE REQUIREMENTS FOR THE DEGREE OF **Master of Science**.

Chief Michael Gossman, M.S., DABR, FAAPM
Thesis Co-director

Brent Foy, Ph.D.
Thesis Co-director

Committee on Final Examination

Chief Michael Gossman, M.S., DABR, FAAPM

Doug Petkie, Ph.D.
Chair, Department of Physics

Brent Foy, Ph.D.

Thomas Skinner, Ph.D.

Robert E. W. Fyffe, Ph.D.
Vice President for Research and
Dean of the Graduate School

ABSTRACT

Courter, Erik J. L. M.S. Department of Physics, Wright State University, 2016.
Use of ClearView Gel Dosimeter for Quality Assurance and Testing of Stereotactic Radiosurgery

There exists a lack of accurate, reproducible three-dimensional dosimetry techniques for stereotactic radiosurgery (SRS) commissioning and quality assurance. This experiment evaluates the use of ClearView gel dosimeters as an alternative to current methods for small field dosimetry in SRS testing. ClearView differs from other gel dosimeters in that it uses tetrazolium salt in its chemical make-up in place of traditional Fricke-type compounds. Using a Varian TrueBeam radiotherapy system to deliver the radiation, three vials of ClearView gel dosimeter were tested in three different dose delivery scenarios. The first test examined the dosimeter's response to a static beam with the dose isocenter targeted to the centroid of the vial. The second evaluation consisted of a full rotational SRS delivery about thecenter of the dosimeter. Lastly, a complete end-to-end treatment plan was performed to evaluate the accuracy of the dosimeter in a full SRS procedure. The three dosimeters were then scanned to measure the dose distribution throughout the gel. Finally, the resulting datawas compared to the initial treatment plan to determine the

accuracy of the gel. According to the comparisons performed, the ClearView gel showed capability of sub-millimeter spatial accuracy across the three evaluations, with a maximum geometric uncertainty of 1.2 mm. Based on these results, ClearView gel showspromise for possible use in SRS dosimetry applications in clinical settings.

TABLE OF CONTENTS

TABLE OF CONTENTS (CONTINUED)

TABLE OF CONTENTS (CONTINUED)

LIST OF FIGURES

Figure **Page**

LIST OF FIGURES (CONTINUED)

FigurePage

LIST OF TABLES

TablePage

1.0 INTRODUCTION

Stereotactic radiosurgery (SRS), also known as stereotactic radiotherapy (SRT), is an increasingly common technique for treating intracranial tumors or other small target areas. In SRS, high doses of radiation are delivered with very steep falloffs outside of the target area, saving the healthy tissue surrounding the target [1]. Further advancements in SRS with rotational delivery allow for even more accuracy and target precision for treatment of exceedingly small targets [2].On average, typical prescribed doses can range from 15 – 21 Gy for SRS treatment of cancerous tumors within the brain, with individual beams of up to 50 Gy [3, 4]. With this high amount of dose being delivered to such concentrated areas, it is of great importance that the treatment dose be accurately delivered only to the target area for the safety of the patient.

In order to ensure accurate, safe patient treatmentwith stereotactic radiosurgery, a quantifiable form of dose measurement is crucial in the commissioning processfor SRS systems [5]. Commissioning is the first step in determining the viability of a new SRS system after installation, which examines four basic areas of SRS: precision, localization, dose distribution, and patient safety [6].A test of precision determines whether or not the system is able to hit the target area within an established amount of spatial uncertainty calculated for the machine. Localization can then be verified by ensuring that the dose delivered to the target does not exceed the target area. Within this area, dose distribution

can be examined to determine how the dose of the system would be distributed in human tissue. Finally, patient safety is carefully monitored throughout the testing procedure to ensure that no extraneous dose is delivered and outside sources of interference are limited. After these four properties of a new SRS system have been deemed acceptable by a Qualified Medical Physicist, the system must then be continually tested to ensure that the machine stays within the acceptable limits, a process known as Quality Assurance (QA) [7].

QA tests are essential to SRS systems in order to reduce accidents as well as identify possible sources of errors in treatments, so the methods to evaluate these systems must have the capability to examine every aspect of SRS treatment in question [7]. As stated earlier, SRS systems have the capability to rotate about very small target volumes during delivery of very high doses. Due to this unique property of SRS treatments, the resulting dose distribution can become difficult to quantify accurately, requiring an extensive quality control procedure to ensure SRS accuracy [7, 8, 9, 10].

An integral part of the quality control procedure is the choice of the radiation detector used for dose determination. Several different types of two-dimensional(2D) detectors have been utilized for SRS, including ion chambers, radiographic films, and semiconductor detectors [4, 11, 12, 13]. An overview of the usability and accuracy of several detector types will be briefly discussed in the following section.

1.1 Traditional2D Detectors

1.1.1 Ion Chamber

Perhaps the most traditional type of 2Dradiation detector used for SRS dosimetry is the ionization chamber. Typical ion chambers consist of two electrodes across a voltage gradient separated by a gas-filled cavity inside the chamber. Incoming ionizing radiation creates ion pairs within the gas, causing a flow of charge when the charged ions are accelerated to the oppositely-charged electrodes. This flow of charge can then be measured to quantify the amount of incoming ionizing radiation.

In the past, ion chamber size has been a limiting factor for SRS applications, with physical diameters too large for the small field sizes utilized in SRS treatments [8, 14].When the diameter of the detector is comparable to the field size used in SRS delivery, precise determination of the dose isocenter location can be difficult if even possible without averaging.However, the development of micro ion chambers has improved the usability of ion chambers for SRS systems, though averaging can still occur [4, 15], allowing measurement of dose distribution in smaller fields. Additionally, both ion chambers and micro ion chambers suffer from a lack of spatial resolution for the high dose falloffs and intensities required in SRS dosimetry [4, 16].

Finally, another difficulty when using ion chambers for SRS QA is how the beam interacts with the gas medium inside the ionization chamber itself. Since human tissue is much more equivalent to water than air, certain ion chambers differ fundamentally in the

reported dose rate to the dose that would be received by tissue [8]. Therefore, an extra step must be applied to correct for this difference after the data has been acquired.

1.1.2 Radiographic Film

Another common detector for current SRS QA methods aside from ion chambers is radiographic film. Basic radiographic film consists of an emulsive layer applied to a base with a protective coating sealing the emulsion. Though films can differ greatly in type (single emulsion or double emulsion, intensifying screen or non-intensifying screen), common films interact with incoming ionizing radiation through the emulsion applied on the base. Silver halide crystals suspended within the emulsion interact with the incoming radiation and store the energy until the film is developed. The dose data from the developed film can then be determined through measuring optical density (OD).

Radiographic films offer much higher spatial resolution than most ion chambers, which is beneficial due to the steep dose gradients used in SRS treatments [4, 8, 17].However, non-reproducibility is a problem for some applications using radiographic films [4, 8, 15]. Reproducibility is limited for radiographic films dues to several factors during manufacturing and exposure to radiation. Films can differ individually due to inhomogeneities during the manufacturing process, during which crystals in the emulsive layer are randomly distributed across the film. This distribution can lead to slight variations in interaction to incoming radiation which in turn leads to different OD readings after development. Air pockets inside the protective packaging to shield the film from external light can also cause inhomogeneities in OD readout [15]. Finally, film orientation in relation to the source also contributes to reproducibility of radiographic

films in SRS. Though these limitations can be overcome or simply deemed negligible in medical imaging procedures, they are too great for consistent use in small field dosimetry, especially in SRS commissioning and QA.

1.1.3 Semiconductor Detectors

Semiconductors such as diode detectors and metal oxide semiconductor field effect transmitters (MOSFET) have also been used for SRS dosimetry. Semiconductor detectors offer small size and can be arranged in arrays for increased spatial resolutions, and they offer real-time data acquisition [10, 15, 18]. Unfortunately, diode detectors suffer from temperature dependence and directional dependence in relation to the source.Also, much like radiographic films, both diode detectors and MOSFETs suffer from reproducibility issues as well due to orientation in relation to the source [14, 15]. Tissue equivalency is also a disadvantage shown by diodes much like ion chambers [8, 18].

Recently, a new type of semiconductor detector has emerged for SRS dosimetry: diamond detectors. Developments in production of synthetic diamond have allowed for the production of small synthetic diamonds for use in dose measurement systems in place of silicon diodes [10]. Although diamond detectors can be considered soft-tissue equivalent and energy independent, they have the issue of being dose rate dependent, requiring calculated corrections to account for this dependence [8, 10].

1.1.4 Thermoluminescent Dosimeters

Thermoluminescent dosimeters (TLD) are another radiation detector type used for dosimetry in clinical applications. This detector type reacts with ionizing radiation by emitting light proportional to the amount of energy received by the incoming radiation. TLDs can be created in small sizes and arranged in arrays much like diode detectors, allowing for a high spatial resolution [19].Some types of TLDs also are largely tissue equivalent, which allows for closer simulation ofhow dose would be distributed in human tissue during treatment [14, 18]. The biggest problem with TLDs is that, similarly to both films and semiconductors, TLDs suffer from issues in reproducibility and consistency[8, 14].

1.2 Gel Dosimeters

All of the above detectors each have individual benefits for use in SRS commissioning and QA.However, one large drawback to all of the above detectors is their ability to only capture data in two dimensions.Many detectors, such as ion chambers, radiographic films, and diodes also are highly dependent on the incoming beam energy, with films, diodes, and diamond detectors also affected by the rate at which the dose is being delivered [8, 14, 15]. In addition, some of the above detector types are limited in the amount of dose that they can measure.

For these reasons, gel dosimetry has emerged as a promising method for ensuring three-dimensional SRS dose accuracy [9, 11, 20, 21]. The ability to measure dose delivery in three dimensions allows for precise determination of the isocenter from the machine's output. Currently, two main types of gel dosimeters are common for this purpose, and they will be explored here.

1.2.1 Fricke Gel Dosimeters

In 1927, Fricke explored early chemical dosimetry dealing with ferrous-sulphate solutions for radiation detection [22]. When irradiated, the ferrous Fe^{2+} ions embedded in the solution will transform into ferric Fe^{3+} ions [22]. After the emergence of three dimensional imaging techniques such as nuclear magnetic resonance imaging (MRI), Gore proposed further developing Fricke's techniques to obtain dosimetry for three dimensional applications [23, 24]. To accomplish this, aqueous Fricke-type solutions were fused into gels to form three dimensional gel dosimeters, which could then be scanned by MRI techniques to obtain dosimetry information [25].

In addition to MRI interpreted results, xylenol orange is now commonly added to the Fricke-typegel solutions as a different data technique. These Fricke-types of dosimeters will develop a visible color change upon irradiation and subsequent Fe^{3+} ion production [26]. This visible color change can then be scanned asOD measurements, which exhibits a linear relationship with the amount of dose received by the gel [27]. These types of Fricke gels are convenient in that they can be imaged on site at clinics where MR imagers are not present [24].

Fricke-type gel dosimeters originally suffered from a disadvantage of low sensitivity, with linear responses up to approximately 10 Gy [25, 27]. However, doses of up to 40 Gy may result in linear dose relationships if the gel is purged with oxygen prior to irradiation [28]. This limitation poses a problem for modern SRS techniques, in which

higher doses may be delivered during treatment. Additionally, chemical instability of Fricke gels poses another issue for dosimetry, which causes a degradation of the retained dose information over time [29]. The diffusion of the Fe^{3+} ions after irradiation eventually destroys the spatial resolution contained by the gel [24]. In order to overcome these limitations, physicists and chemists alike are exploring the development of other types of gel dosimeters. In addition to the development of polymer gel dosimeters as discussed below, another type of gel dosimeter based on the chemistry of tetrazolium salts, ClearView, will be discussed later in section 1.2.3.

1.2.2 Polymer Gel Dosimeters

Another type of common gel dosimeter is a polymer gel dosimeter, which will be briefly discussed here. Polymer gel dosimeterswere first discussed well after the emergence of Fricke-type gels. The first step in polymer gel dosimetry occurred in 1957 when works by Andrews examined the effects of ionizing radiation on polymethylmethacrylate [30]. Following this study, investigations into polymers for dosimetry showed promise for development of a polymer-type dosimeter.In 1992, a new type of polymer gel dosimeter under the acronym BANANA emerged, named after its chemical makeup (bis, acrylamide, nitrous oxide, and agarose) [20]. Later, the agarose component was replaced with aqueous gelatin under the generic acronym PAG.

Polymer gels exhibit high reproducibility in terms of dose response and distribution and also have the capability of minimal dose rate dependence [31]. Unlike Fricke-type dosimeters, these gels use the properties of radiation-induced polymerization and cross-linking of acrylic monomers and in turn do not suffer from the diffusion

problem associated with Fricke gels [11, 20]. However, oxygenation issues posed a problem for early polymer dosimeters, requiring the dosimeters to be manufactured in an oxygen free environment. This issue was later remedied by a new formulation of polymer gels under the acronym MAGIC (methacrylic acid, ascorbic acid, gelatin, and copper), though limited studies have looked into their use for dosimetry over Fricke-type gels [20].

1.2.3 ClearView Gel Dosimeter

The dosimeter used in this experiment is ClearView gel dosimeter by Modus Medical Devices, Inc. (Ontario, Canada). As stated previously, ClearView differs from other gel-type dosimeters in that it is based on tetrazolium salt chemistry, which was originally conceived for use in liquids and films. The composition of the gel features less than one percent of the tetrazolium salt suspended within glycerol (10 vol. %) in water with a gellan gum gelling agent (1.25 wt. %). This combination of compounds results in a gel with a physical density of 1.02 g/cm^3, which is very close to the density of water.

Due its specific composition, this new type of gel exhibits a strong linear relationship between absorbed dose and OD of the irradiated gel within ranges of 10-80 Gy. This useful range of linear operation is much wider than the ranges for Fricke-type gels as discussed in the introduction, giving ClearView a much more flexible use for SRS treatments. Within this established dose range, higher doses will result in a higher signal to noise ratio, with an optimal performance range across the middle of the spectrum.

Upon irradiation, the ClearView gel will exhibit a purple hue proportional to the dose received, with doses of more than 20 Gy resulting in a change visible to the eye. The more radiation the gel receives, the darker the shade of purple the gel displays. This color change is due to the chemical formation of a formazan dye within the gel upon ionization. Increased radiation absorption correlates directly to an increased formation of the dye, hence the deepening of the purple shade after more intense irradiation. A manufacturer recommended development time of 45 minutes after irradiation ensures that the dose information stored in the dye has time to fully darken in areas where dose has been concentrated. The development process does not require any additional work by the user, just that the gel be allowed to remain at room temperature during the 45 minute period as the chemical reactions in the gel stabilize.

Once irradiated, the purple shade will remain permanently fixed in place within the gel, thus retaining all of the information regarding dose applied to the dosimeter. Due to this permanent change, each vial of ClearView gel is designed for a single use. Though spatially and chemically stable, biological contaminants may form in the gel over time, so it is best that analysis be conducted within a timely manner after irradiation. Formation of these contaminants can be limited by keeping the gel in chilled containers during shipping and storage, though irradiation of the gel should occur after the gel has warmed to room temperature. The irradiated gel can then be scanned at the manufacturer's facility using an opticalcomputed tomography (CT) scanner to interpret the OD values of the gel and relate them to the amount of ionizing radiation received.

This experiment will examine several factors of ClearView gel such as its response to dose delivery and its capability for high spatial resolution in SRS QA. Other aspects such as energy dependence, dose rate dependence, temperature dependence have been untested at the time of this experiment, but pose viable options for future research.

2.0 MATERIALS AND METHODS

2.1 Planning

For this experiment, three vials of ClearView gel dosimeter were provided from Modus Medical Devices, Inc. With these three dosimeters, the goal was to create and carry out three effective tests to examine the use of ClearView as a clinical gel dosimeter for commissioning and quality assurance in SRS. After several different possibilities were examined, three different scenarios were selected to test the gel's capabilities as an effective dosimeter.

The first evaluation would serve to test the gel's accuracy of dose distribution for a simple, static electron beam targeted through the center of the vial. Since the optimal range of the gel was centered near 40 Gy as discussed earlier, the plan was to deliver a total matching isocenter dose of 40 Gy to the first dosimeter. The results of this irradiation would then show how the dosimeter reacts to dose delivery with minimal outside factors influencing the irradiation.

The second evaluation of the ClearView gel would expand upon the first evaluation's 40 Gy static delivery. However, in this evaluation, the static beam would be replaced by a rotational delivery technique.As discussed earlier in the introduction, new

SRS systems possess the ability to rotate about the target in a 360 degree arc. The treatment plan would utilize this feature to irradiate the gel in a full rotation about the second dosimeter to deliver the 40 Gy dose.

With the first two evaluations examining the gel's performance with basics of SRS dose delivery, the third evaluation should then examine a more in-depth treatment plan. To accomplish this, it was decided that a full end-to-end SRS treatment test would best explore the possibility of using ClearView gel dosimeters for clinical commissioning and quality assurance. Again, a 40 Gy dose would be delivered for consistency across my evaluations, though the methods to deliver this dose would shift as needed to account for the newly-introduced patient geometry and density.

In order to most accurately perform the end-to-end test, it was essential to simulate the physical make-up of a human patient. To accomplish this, a Phantom Laboratory, Inc. (Salem, NY) Model TLP290 RSVP Phantom II head phantom was utilized, which could be filled with water to simulate human tissue for SRS purposes [32]. With proper positioning, a vial of ClearView at a fixed position within the water-filled phantom could accurately simulate anintracranial condition. Since intracranial tumors are commonly treated using SRS systems, it was decided to simulate a left-sided acoustic neuroma by positioning the dosimeter appropriately within the phantom [33].

2.2 Preparation

Upon receiving 3 vials of ClearView gel from the manufacturer, each of the sealed vialswas removed from the chilled shipping container and allowed to warm to

room temperature. The vials measured 8.5 cm in length and 4.3 cm in diameter, and each vial had a wall thickness of 1.0 mm.

Figure 2: ClearView gel dosimeter and adapter

Once the vials had warmed to room temperature as required,the acrylic positioning adapters, which had become disconnected during shipment, were re-attached tothe top of each vial. To re-attach each acrylic adapter to the jar lids, a quick-dry epoxy was used aftereach of the adapters was carefully aligned to match with the original positioning markings on the lid.

2.3 Procedure

2.3.1 Evaluation 1

For the first of the three evaluations, it was decided that a static beam be delivered through the centroid of one ClearView vial. The jarwas first mounted to a CIVCO

Medical Solutions (Orange City, IA) 20-CFHN-SUB2 Type-S™ Overlay Board to prevent movement during the procedure.

Figure 2: CIVCO Type-S™ Overlay Board with attached headrest

Once attached, the board was then placed into a General Electric (Fairfield, CT) LightSpeed RT CT scanner couch. Initial alignmentof the vial was conducted by manually aligning the built-in planar positioning lasers to intersect at the visual center of the vial. Using a 120 kVp scan at 10 mA, a quick "scout" scan was performed to verify proper placement of the vial. Once positioning was satisfactory, a full helical CT scan of the headrest at 120 kVp and 350 mA at 1.25 mm increments was performed. A total of 133 images were collected in a time of 46 seconds through a 17.5 mm cone beam.

The imaging data from the CT scan was then sent to the Varian Medical Systems, Inc. (Palo Alto, CA) Eclipse treatment planning system v11.0. This system allowed for automatic identification of the scanned object in all three planes: axial, coronal, and sagittal. Once the appropriate contour of the vial had been identified, the center of the dosimeter was set to the origin of the planes. Through this central region, a single pencil beam was assigned to pass through the vial in the Varian Cone Planning software. The

beam was designated to be a 6 MV Flattening Filter Free (FFF) beam through a 17.5 mm cone. A total dose of 40 Gy to the vial isocenterwas planned to be delivered for a beam-on time of 4321 MU. The axes of the jar in relation to the beam source are illustrated in Figure 3 below.

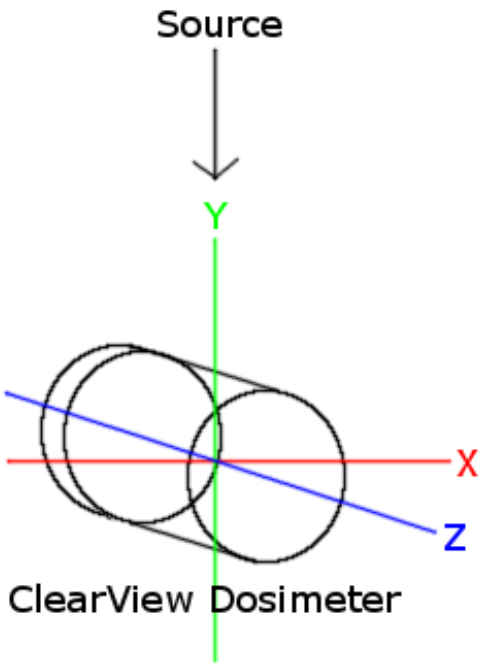

Figure 3: Evaluation 1 ClearView dosimeter axes

Once the treatment planning had been completed, the secured vial was transferred to the Varian TrueBeam particle accelerator. Again, utilizing three planar lasers to position the vial, the visual center of the vialwas set at their intersection. A cone of 17.5 mm in diameter was attached to the particle accelerator and placed into the path of the beam. The room was then cleared, and one static beam was delivered according to the treatment plan. Upon completion of beam delivery, the vial was removed from the

overlay board and allowed to develop for 45 minutes as mentioned previously before being returned to its chilled container.

2.3.2 Evaluation 2

The next evaluation differs fundamentally from the first in that, instead of a single static beam, two 180 degree arc beams were implemented as discussed earlier. First, the second ClearView jar was mounted to the CIVCO board in the same fashion as in Evaluation 1. This assembly was then inserted into the GE LightSpeed CT scanner for initial imaging. Again, visual alignment of the vial's center into the intersection of the three beams' paths ensured that the dosimeter was properly positioned in the scanner. To create a treatment plan, the vial was imaged at 120 kVp and 350 mA at 1.25 mm increments along the length of the jar. As before, a total of 133 images were collected in a time of 46 seconds through a 17.5 mm cone beam. This data was then networked to the Varian Eclipse software for treatment planning.

Once in the treatment planning system, the images were again aligned so that the origin of the three planes was aligned on the center of the ClearView vial. For this evaluation, two 6 MV FFF beams arcs were programed to rotate around the vial. One beam was set to rotate clockwise about the jar from 0 to 180 degrees; the other followed a 180 degree rotation from center in the counter-clockwise direction to encompass the vial entirely between the two beams. Each beam's path around the dosimeter is shown in the following illustration.

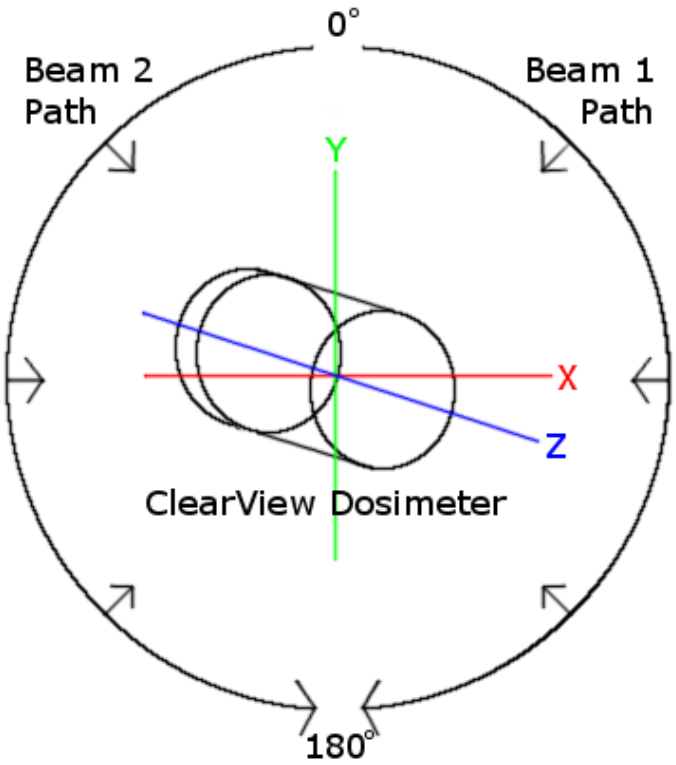

Figure 4: Evaluaton 2 ClearView dosimeter axes

These two beams were set to deliver a combined total dose of 40 Gyto the isocenter through a 15 mm cone. With a successful planning session, the finalized plan was exported to the TrueBeam console in preparation for delivery.

The 17.5 mm cone from the first evaluation was removed and replaced with a 15 mm diameter cone to match the new treatment plan. The vial assembly was then placed onto the accelerator's couch in the path of the visual lasers. Using the intersection of the three planar beams, the vial was carefully centered under the accelerator. Once the vial had been aligned properly, the room was cleared, and the treatment plan was administered. Each of the two arc beams delivered their planned dose for an individual beam-on time of 2249 MU each. After the beams had delivered their dosage,the vial was

detached from the mount, allowed to develop at room temperature for 45 minutes, and then returned to the chilled container.

2.3.3 Evaluation 3

For the final evaluation, an end-to-end test on the ClearView gel was performed, making use of a simulated patient geometry and physical density. To accomplish this, aPhantom Laboratory, Inc. RSVP Phantom II head phantom was utilized, which was filled with water to simulate human tissue as discussed in the introduction.

Figure 5: Phantom Laboratory head phantom

After filling the phantom with water, preparation of the remaining ClearView gel dosimeter began. First, three titanium fiducialswere placed around the surface of the jar for planar identification in the treatment planning software. Then, a plastic rod was attached at the threaded acrylic adapter. This rod assembly was inserted into the base of the phantom at the neck. Finally, the dosimeter was positioned within the phantom to

simulate the left-sided acoustic neuroma according to the planned procedure. The phantom was then sealed water-tight to prevent formation of air pockets within the head.

With the dosimeter securely fixed within the phantom, the phantom was attached to a Varian Head Frame SRS halo through use of four cranial screws. This head frame allowed secure attachment of the head assembly to the couches of both the CT scanner and TrueBeam accelerator. Once attached to the CT couch, three additional fiducials were positioned along the surface of the phantom at the intersections of the wall-mounted positioning lasers. Now, with a frame of reference for the treatment plan, it was time to perform the CT scan. At 120 kVp and 350 mA, 149 images were obtained from the helical scan at 1.25 mm increments in 51.3 seconds. This image set was then sent to the Eclipse treatment planning software.

Using the two sets of fiducials to align the reference planes, the vial was contoured, andthe planned dose isocenter was designated to its center. The Cone Planning software allowed for creation ofa plan of four 6 MV FFF beams delivering a 40 Gy dose to the ClearView dosimeter isocenter. Using specific gantry rotations in addition to couch alignment, these beams were programmed to deliver their dose to the pinpoint target of the vial isocenter with spherical dose falloff. The beam plans are outlined in the following table using standardized coordinates for table position and gantry rotation [34].

Beam	Table Position	Gantry Rotation	Beam-on Time
Arc 1	340°	30°-120°	1819 MU
Arc 2	305°	30°-120°	1818 MU
Arc 3	20°	240°-330°	1462 MU
Arc 4	55°	240°-330°	1574 MU

Table 1: Evaluation 3 beam plan

With these four equally weighted beams, the Varian Aria record-and-verify system performed a cone-beam CT (CBCT) before treatment delivery to ensure correction of any inaccuracies in phantom alignment on the TrueBeam six-degree of freedom (6DOF) couch. This treatment plan was finalized and sent to the TrueBeam console.

The phantom assembly was transferred from the LightSpeed CT scanner to the TrueBeam 6DOF couch. Using the visual alignment lasers to position the phantom under the center of the accelerator, the phantom was carefully attached to the 6DOF couch.

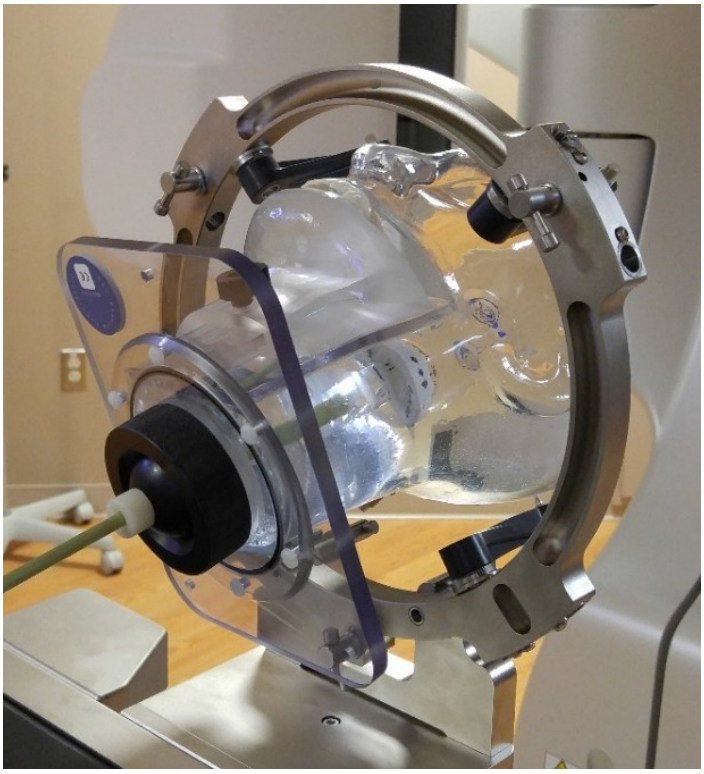

Figure 6: Phantom assembly secured using SRS halo

Again, the 15 mm cone was used to deliver the beams in this evaluation. With the phantom and ClearView dosimeter in place, the room was cleared in preparation for treatment delivery.

Once the room was closed, the scheduled 120 kVp CBCT commenced prior to dose delivery. Using the 6DOF to adjust as necessary, the system corrected for positioning discrepancies between the treatment plan and the initial placement of the phantom. After the CBCT had finished and the automatic adjustments were made, each of the four beams was delivered according to the finalized treatment plan. Once the treatment was complete, the phantom was removed from the couch and drained. After the water had been drained, he ClearView gel dosimeter was carefully removed from the

phantom and dried. Once developed, the dosimeter was placed with the other two vials in the chilled container.

2.4 Examination

With the three vials securely packed into the chilled shipping container, the package was then shipped back to the manufacturer for scanning. Two days after initial treatment delivery, the ClearView vials were scanned at the Modus facility using a Vista 15 optical CT scanner. This OD scan data was then converted to dose distribution using a calibration scan, which is dependent on manufacturing variation of the gels and thus must be calibrated for each different batch. This calibrated dose information was then imported into the VistaView 3D Visualization Software v.0.3.3 where the distribution can be displayed in three dimensions. Finally, these files were sent back forcomparative analysis within the VistaView software.

2.5Sources of Uncertainty

For each of the three evaluations, several sources of uncertainty had to be taken into account. The systematic uncertainties of the evaluations were accounted for in similar fashion to the studied of AAPM Task Group 42 [R]. For Evaluations 1 and 2, the first source of uncertainty to appear in the trial was the repositioning of the acrylic adapter to the lid of the vial. Though the adapter itself was not attached to anything aside from the lid itself, the markings on the adapter were later used for adjusting scanner alignment at the manufacturer's facility. Since the adapter was to be used for this purpose based on a baseline scan before transit, an attempt to position the 1.0 mm wide markings

on the adapter itself to directly align with the markings on the vial's lid was made. Due to this possible misalignment, an uncertainty contribution of $\delta_1 = 1.0$ mm was accredited to the first evaluations.

The second source of uncertainty taken into account for the first evaluations was the accuracy of the Varian TrueBeam particle accelerator. A Winston-Lutz isocenter test was performed to quantify this uncertainty prior to irradiation. On the day of the evaluations, a 5 cm^3 cube with an internally centered fiducial was placed in the 6DOF couch under the accelerator. This fiducial was then centered under the crosshairs in the light field of the accelerator at several different orientations. From this test, it was determined that an additional uncertainty of $\delta_2 = 0.3$ mm be included for the gantry positioning. Another positioning uncertainty that factors into the final results is the manual alignment of the vial using the wall lasers. Although the placement of the vial between the CT scanner and the TrueBeam was replicated as uniformly as possible, an additional alignment uncertainty of $\delta_3 = 0.25$ mm was accounted for in the final uncertainty calculations.

Finally, after the evaluations had been completed, the manufacturer's reading of the ClearView gel data introduced additional uncertainties into the results. As stated previously, small markings on the lids of the vials were scanned prior to shipment to establish a baseline orientation of the jars within the Vista scanner. When aligning the small markings, a stated uncertainty of $\delta_4 = 0.5$ mm is proposed by the manufacturer. In addition, the wall of the vial itself contributes a significant amount of uncertainty to the final results. When scanning the ClearView vial after the dosage has been delivered,

several factors can have an effect on the output accuracy. Variables such as wall thickness, refractive index, and differences in jar manufacturing can all have noticeable effects on the apparent OD of the gel. With all of these scenarios in mind, a possible uncertainty of $\delta_5 = 1.0$ mm was assigned to the Vista scanner readout.

To calculate the total uncertainty for my data, each of the individual uncertainties from the five sources listed above was squared. Then, the standard deviation by quadrature was found by taking the square root of the sum of all the individual squared uncertainties. This calculation resulted in a total overall uncertainty of $\delta = 1.6$ mm. The sources and results are shown in the following table.

Uncertainty Source	δ (mm)
Acrylic adapter alignment	1.0
Winston-Lutz isocenter test	0.3
Manual laser alignment	0.25
VistaView scanner alignment	0.5
VistaView scanner readout	1.0
Standard deviation by quadrature	1.6

Table 2: Evaluation 1 and 2 uncertainty sources and values

The sources and values in Table 2 apply only to Evaluations 1 and 2. For Evaluation 3, several of the sources are replaced according to the method of delivery. As before, the reattachment of the acrylic adapter introduced an initial uncertainty of $\delta_1 = 1.0$ mm when carefully aligning the markers. Since the adapter was used for attachment of

the vial to the positioning rod in this evaluation, realignment was crucial to obtaining accurate results.

Unlike Evaluations 1 and 2, Evaluation 3 utilized not only the rotational positioning of the TrueBeam gantry, but also the movement of the 6DOF couch. With this additional movement, the Winston-Lutz isocenter test revealed a total uncertainty of $\delta_2 = 0.6$ mm, a 0.3 mm increase over the gantry rotation alone. In place of the manual laser alignment used to position the vials on the first two evaluations, the onboard CBCT was utilized in order to align the isocenter of the dose to the centroid of the vial. This process has a manufacturer specified uncertainty of $\delta_3 = 0.1$ mm for the CBCT and 6DOF couch.

Once again, after the three evaluations had been completed, additional uncertainties were introduced during the dosimeter scanning process at the manufacture's facility. Alignment of the small markings on the top of the vial contributed an alignment uncertainty of $\delta_4 = 0.5$ mm as stated by the manufacturer. Finally, a possible uncertainty of $\delta_5 = 1.0$ mm was assigned again to the Vista scanner readout based on factors of the physical jar containing the ClearView gel. These sources and uncertainties are listed in Table 3 below.

Uncertainty Source	δ (mm)
Acrylic adapter alignment	1.0
Winston-Lutz isocenter test	0.6
CBCT registration	0.1
VistaView scanner alignment	0.5
VistaView scanner readout	1.0
Standard deviation by quadrature	1.6

Table 3: Evaluation 3 uncertainty sources and values

The final standard deviation by quadrature value of δ= 1.6 mm was calculated in the same fashion as stated for Evaluations 1 and 2.

3.0 RESULTS

3.1 Preliminary Observations

Immediately after dose delivery, the purple-shaded formazan dye was clearly visible to the naked eye. As expected, darker shades of purple could be seen closer to the isocenter of the dose delivery [S]. In Figure 7below, the purple dye can be seen to be concentrated in the centroid of the vial.

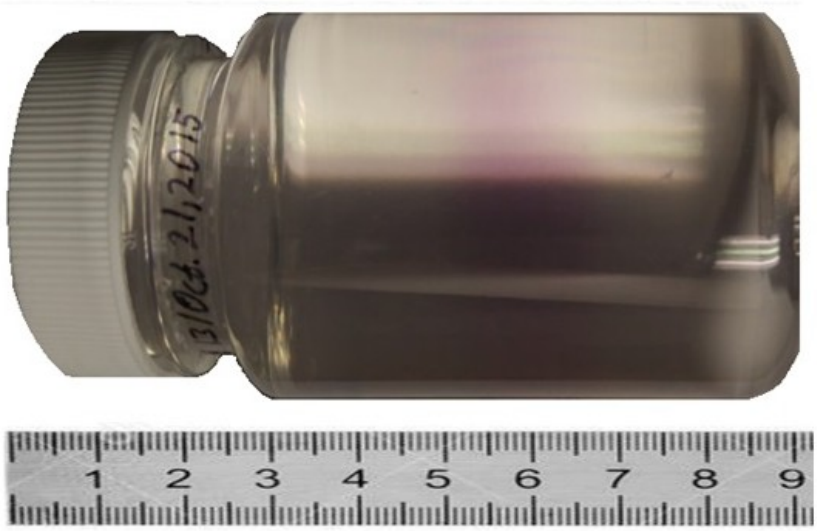

Figure 7: ClearView gel after radiation delivery

3.2Scan Results

3.2.1 Evaluation 1

After receiving the VistaView files from Modus, the scan data was loaded to compare to the original treatment plan. Using the three reference planes (axial, coronal, sagittal), thedosimetry results were analyzed in relation to thetreatment plans used for delivery. For the single beam delivery from Evaluation 1, a side-by-side comparison of

each plane within the VistaView software shows an early visual compliance between the two data sets. The brighter red areas correlate to a higher dose received by the gel, where the blue background indicates a lower or non-substantial amount of radiation.

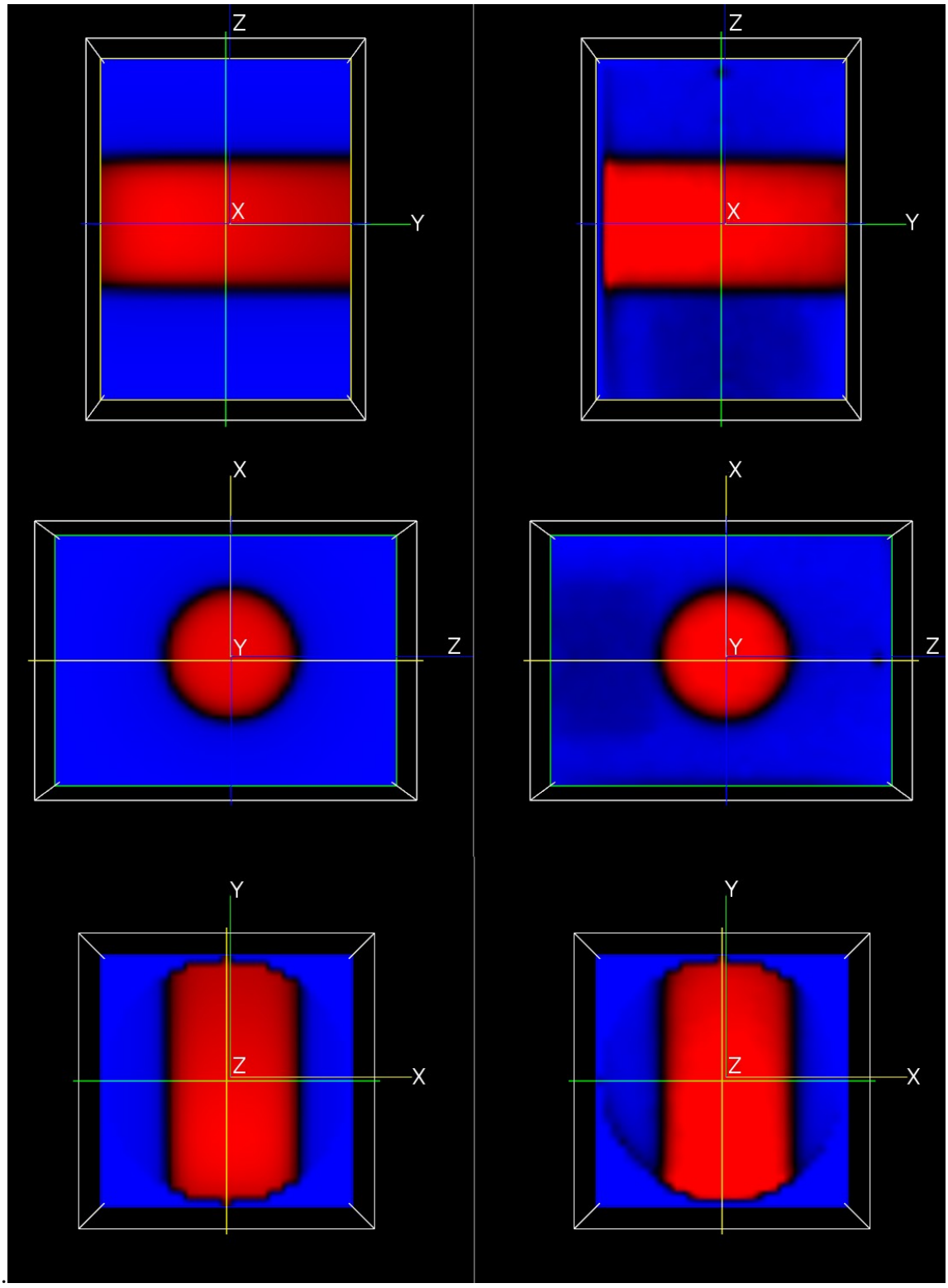

Figure 8: Evaluation 1 planned (left) and measured (right) dose distribution by plane. Top to bottom: sagittal (ZY), coronal (ZX), axial (XY)

From these visual comparisons in Figure 8 above, it is clear that the planned dose and measured dose show similarities in both shape and intensity. In addition to the expected dose distribution surrounding the isocenter, slight dose accumulation in the measured dose planes is visible. However, in order to determine the level accumulated in the shadowed regions and also verify geometric accuracy, line-dose profiles were used within the VistaView software across each axis to quantify the results of the dose distribution. Figures9–11 below show the results.

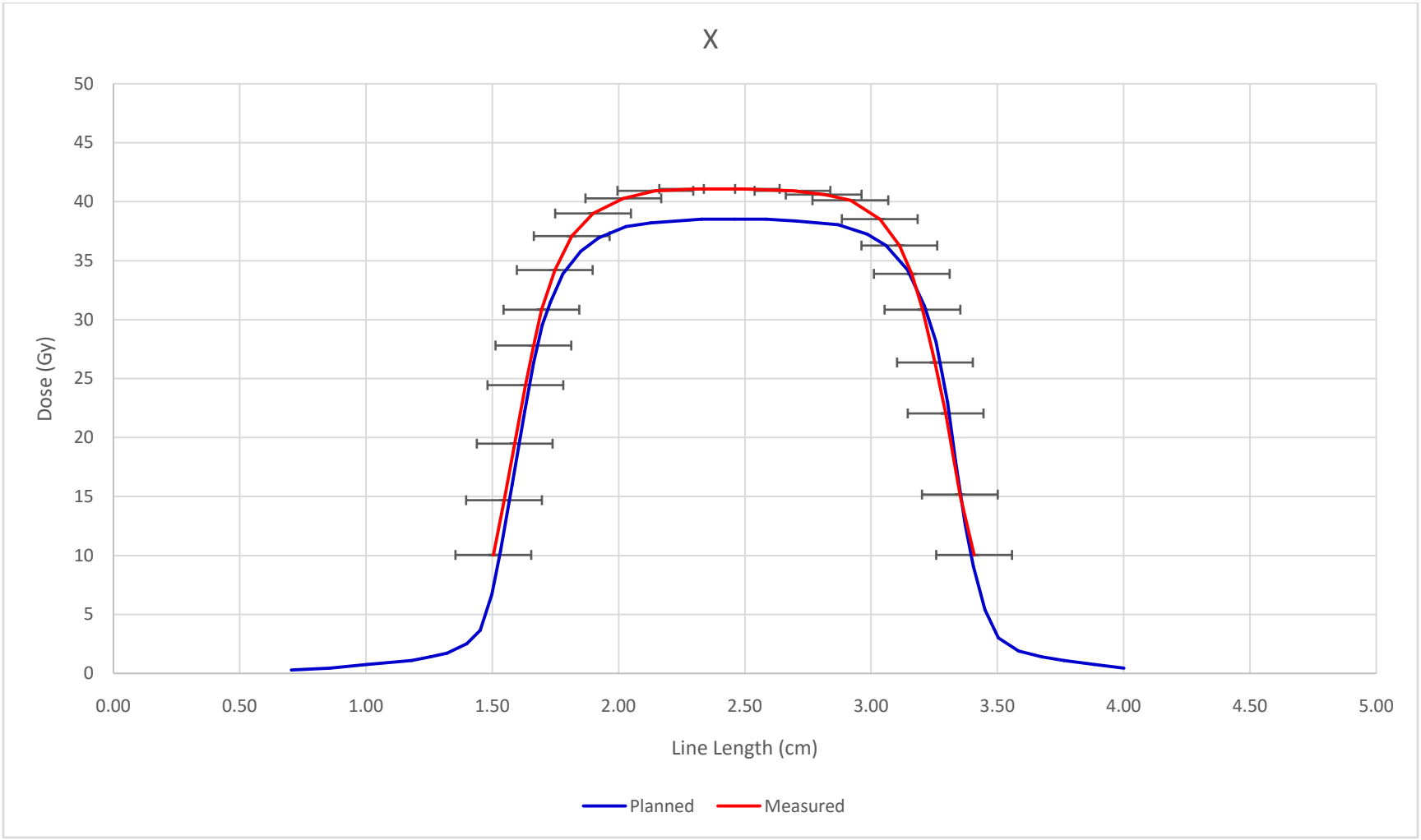

Figure 9: Evaluation 2 X-axis line-dose profile across sagittal plane

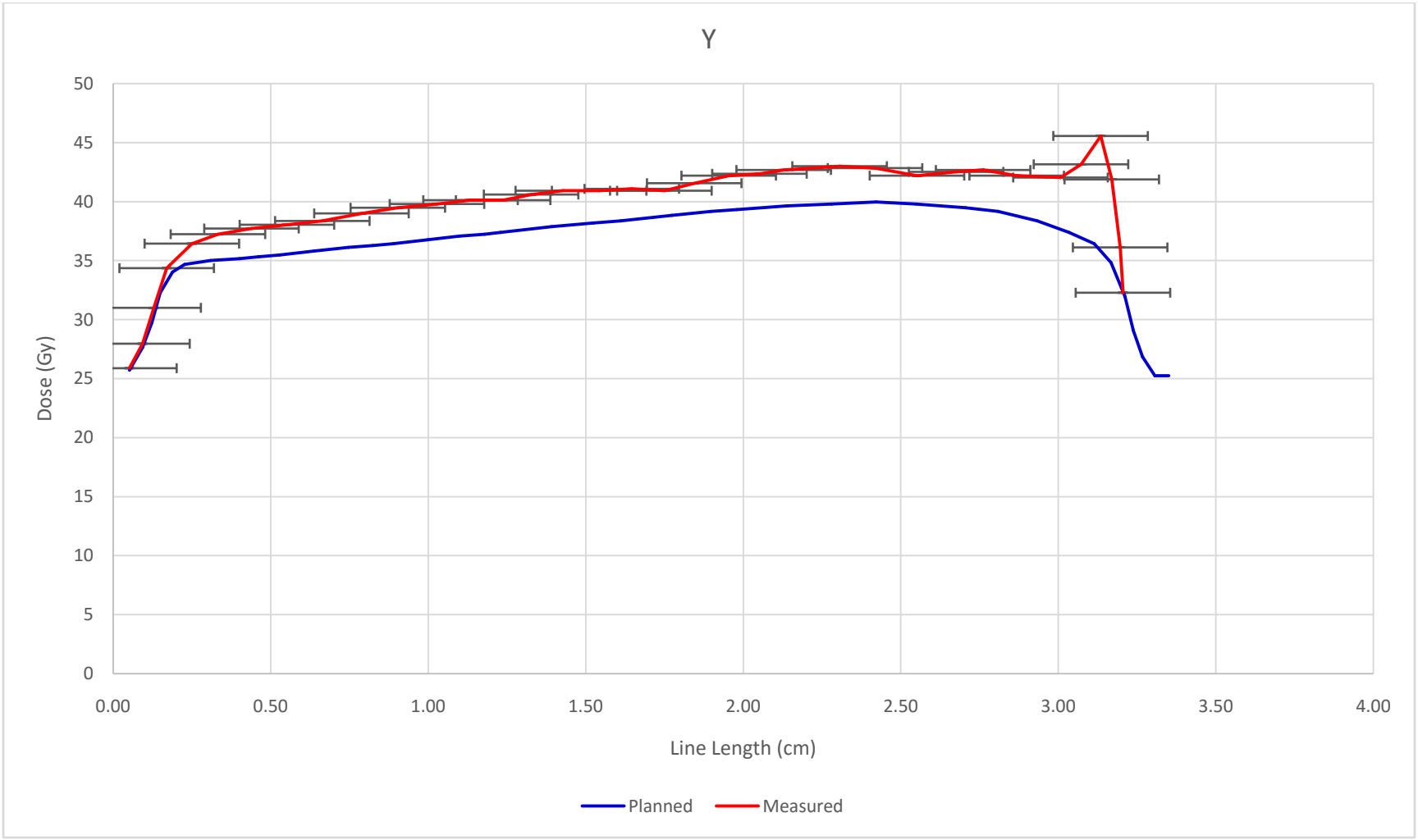

Figure 10: Evaluation 1 Y-axis line-dose profile across axial plane

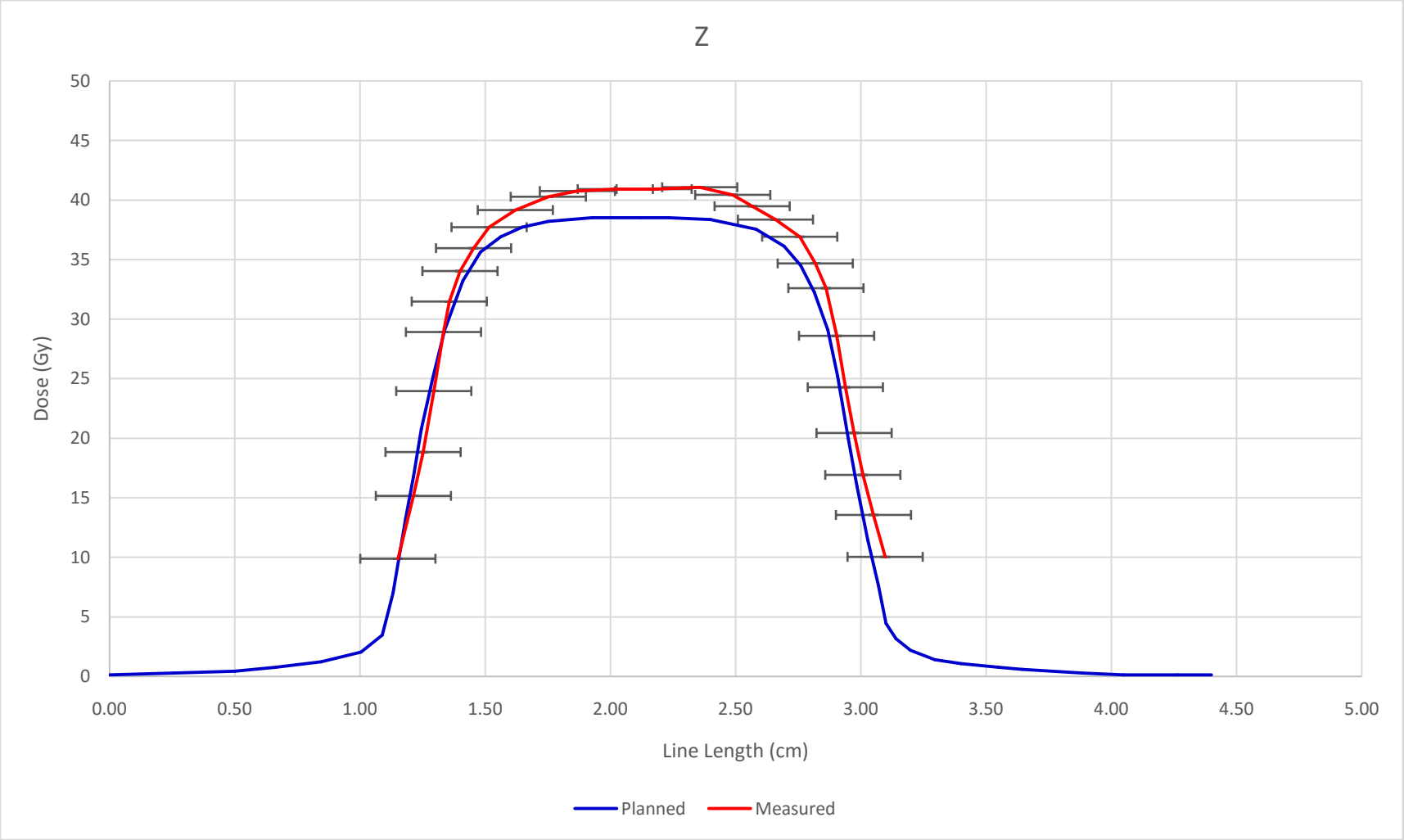

Figure 11: Evaluation 1 Z-axis line-dose profile across coronal plane

For these three figures, the red data set represents the measured values obtained by the ClearView gel through the Vista scanner within its suggested dose range. The blue data set for each figure shows the planned dose across each axis. The error bars along each measured data set show the calculated margin of uncertainty (δ=1.6 mm) for each dose distribution, which was calculated in an earlier section. With the error bars in place, the dose distribution for the ClearView gel dosimeter falls within the range of acceptable values for Evaluation 1.

3.2.2 Evaluation 2

The second evaluation was performed to determine the viability of ClearView gel as consisted of two arc beams delivering equal dosage to the gel. As before, the following figure shows a side-by-side comparison of the planned dose delivery to that recorded by the ClearView gel dosimeter.

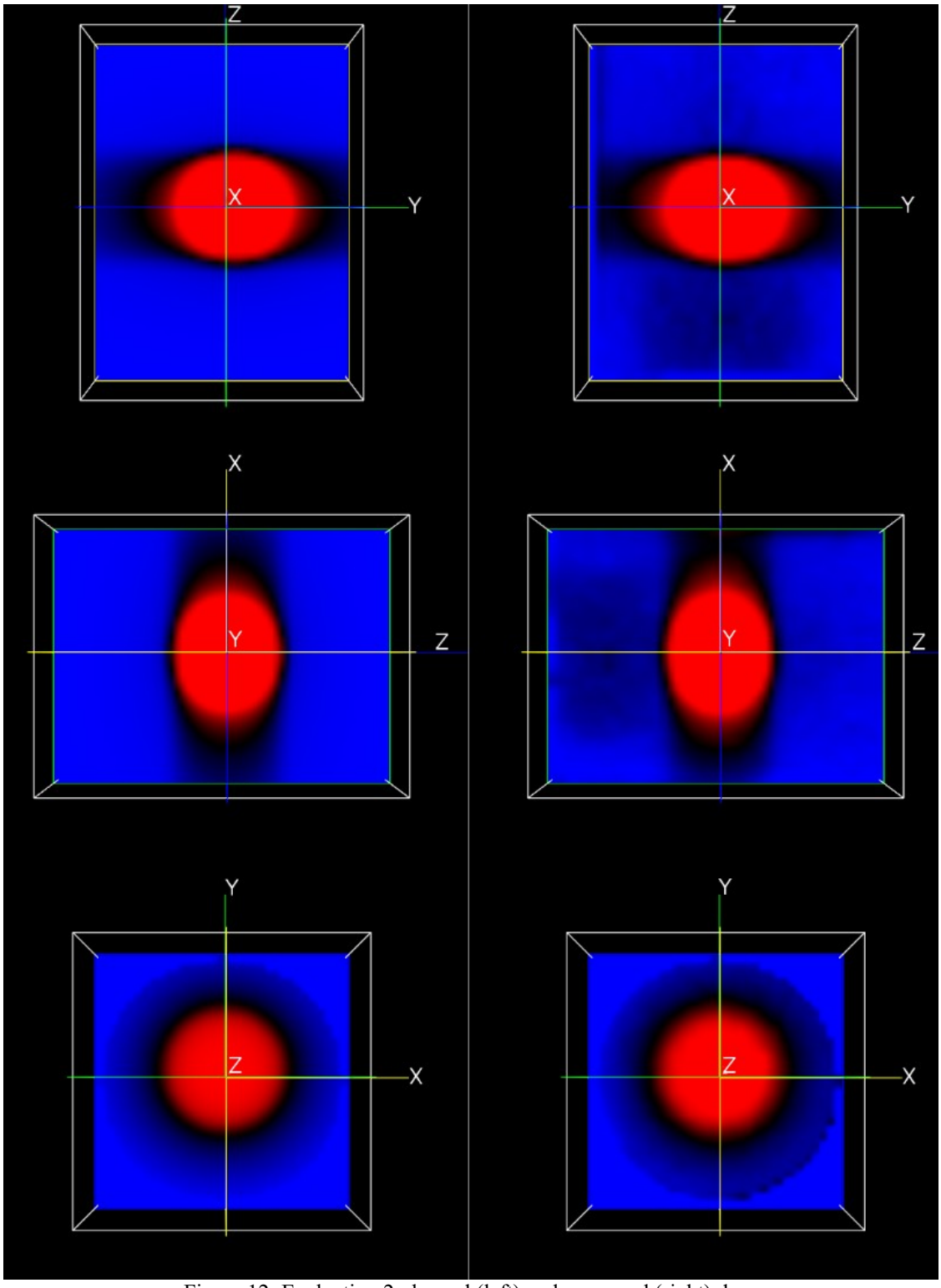

Figure 12: Evaluation 2 planned (left) and measured (right) dose distribution by plane. Top to bottom: sagittal (ZY), coronal (ZX), axial (XY)

Once again, the above figure shows an early visual indication that the two data sets share similar shape and intensity relative to one another. The general shapes ofthe dose distributions between each of the corresponding three planes appear to exhibit the same falloffs and isocenters, with the measured dose planes again showing slight dose accumulation outside the targeted region. From these two data sets, three line-dose profiles were again created for comparison along an axis in each of the three planes.

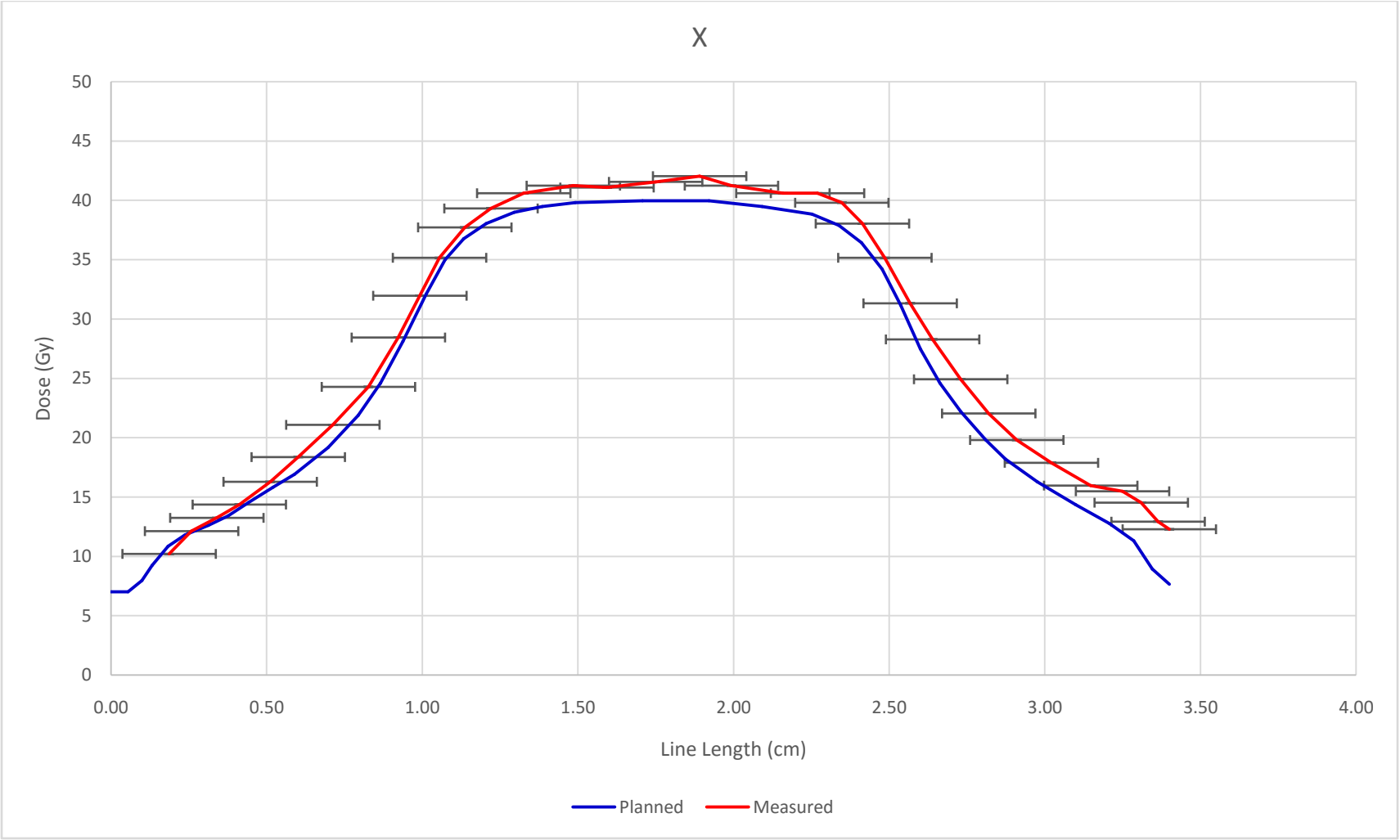

Figure 13: Evaluation 2 X-axis line-dose profile across sagittal plane

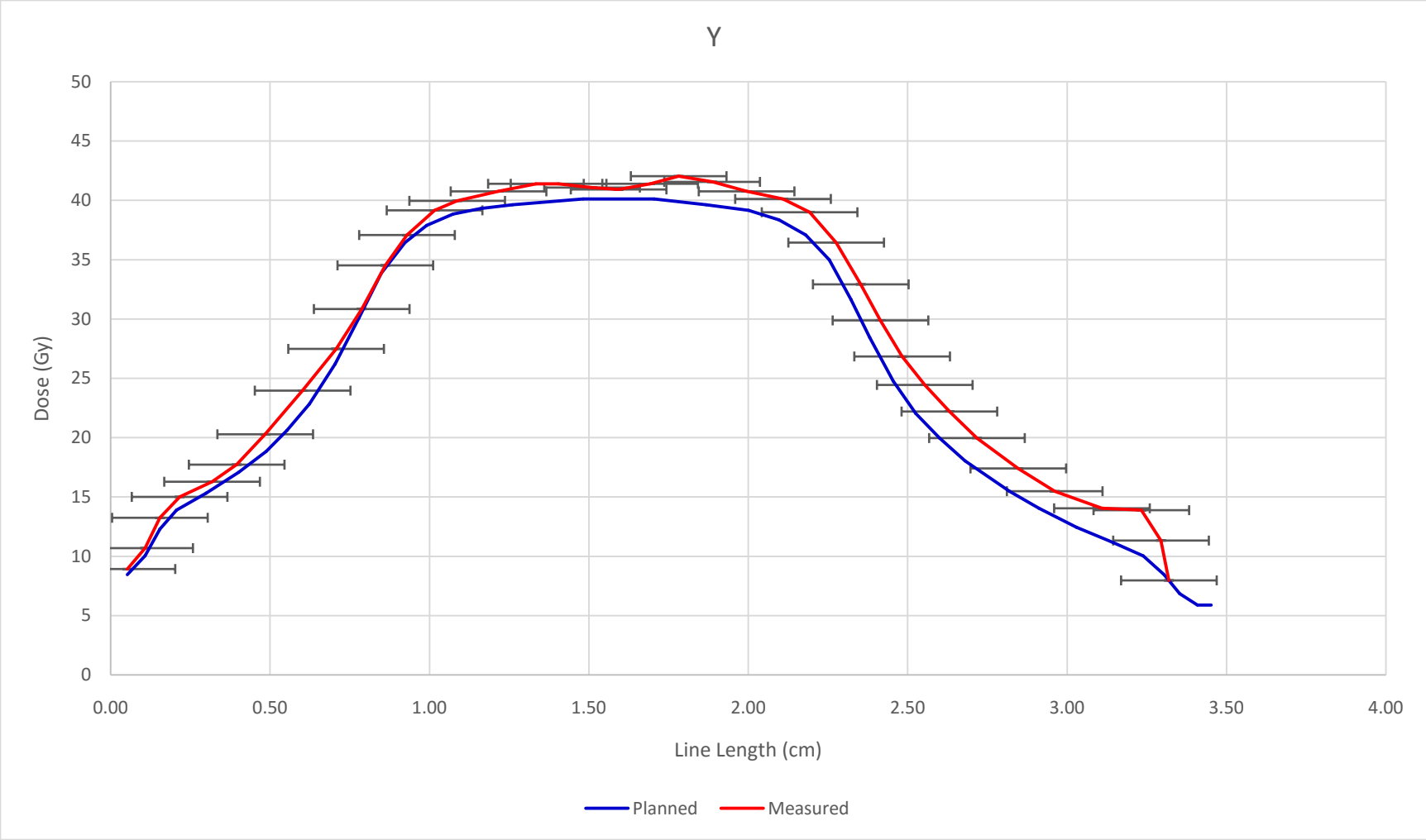

Figure 14: Evaluation 2 Y-axis line-dose profile across axial plane

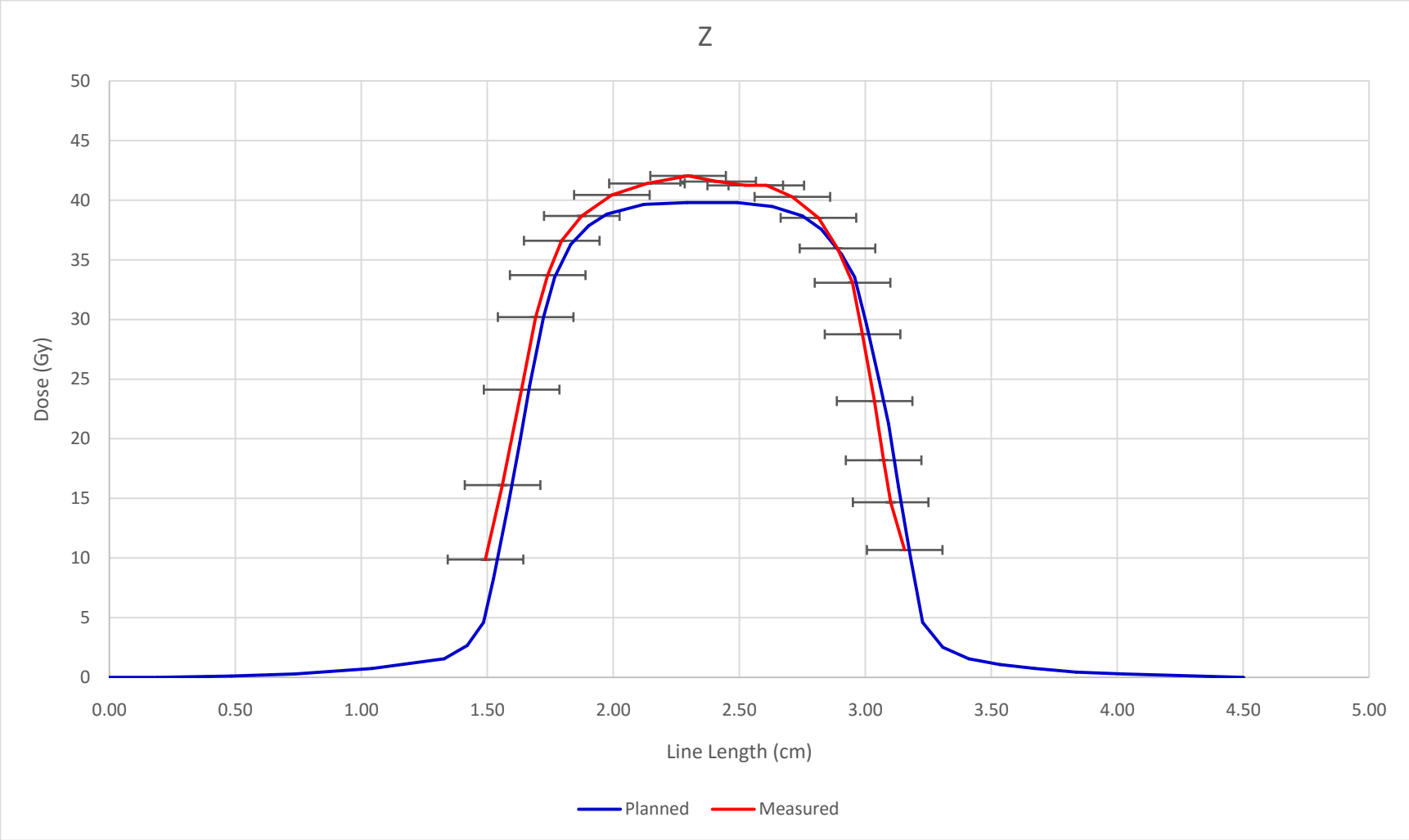

Figure 15: Evaluation 2 Z-axis line-dose profile across coronal plane

With the two arc beams, the results from the dosimeter very closely matched the treatment plan geometrically. As before, the red line represents the ClearView results within its suggested dose range of 10-80 Gy, and the blue line shows the original treatment plan. The error bars above represent the calculated margin of uncertainty (δ=1.6 mm) for each data point along the dosimeter curve.

3.2.3 Evaluation 3

The third and final evaluation of this report examined the use of the ClearView gel in a full end-to-end SRS treatment. Using the same color-coding as in the previous two evaluations, I then measured and planned dose distribution were compared between the two data sets in the VistaView software. Figure 16 below shows the planned dose planes on the left and the measured dose planes on the right.

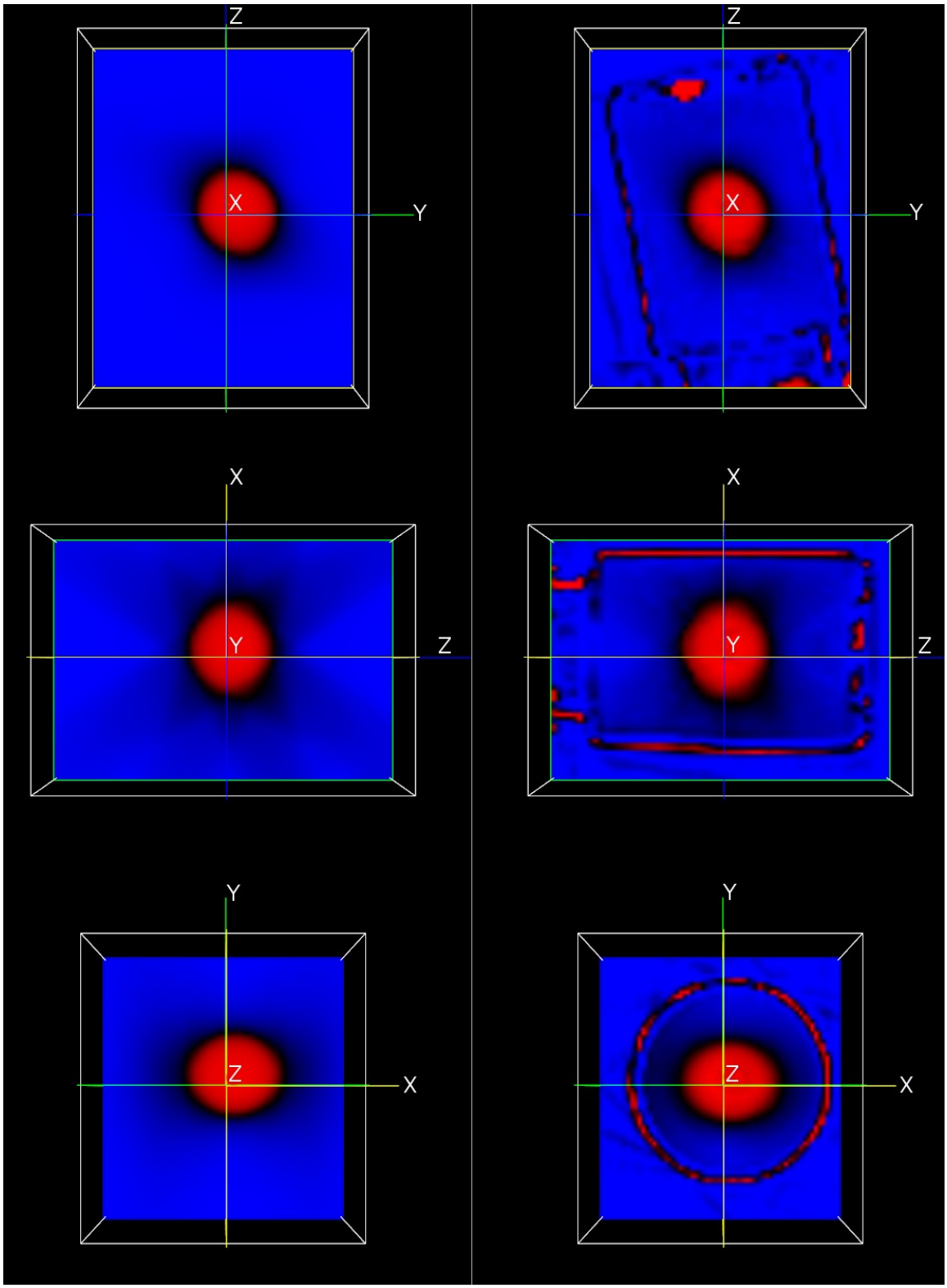

Figure 16: Evaluation 3 planned (left) and measured (right) dose distribution by plane. Top to bottom: sagittal (ZY), coronal (ZX), axial (XY)

The outlines of the jar containing the ClearView gel are purposely present in this evaluation to show the angled positioning of the jar within the head phantom in relation to the three reference planes. Within the jar, the dose distribution can be seen to line up very well, as was the case with both of the previous evaluations. A line-dose profile across each plane can quantify the data to determine accuracy of delivery. The following three plots show the dose distribution in this fashion

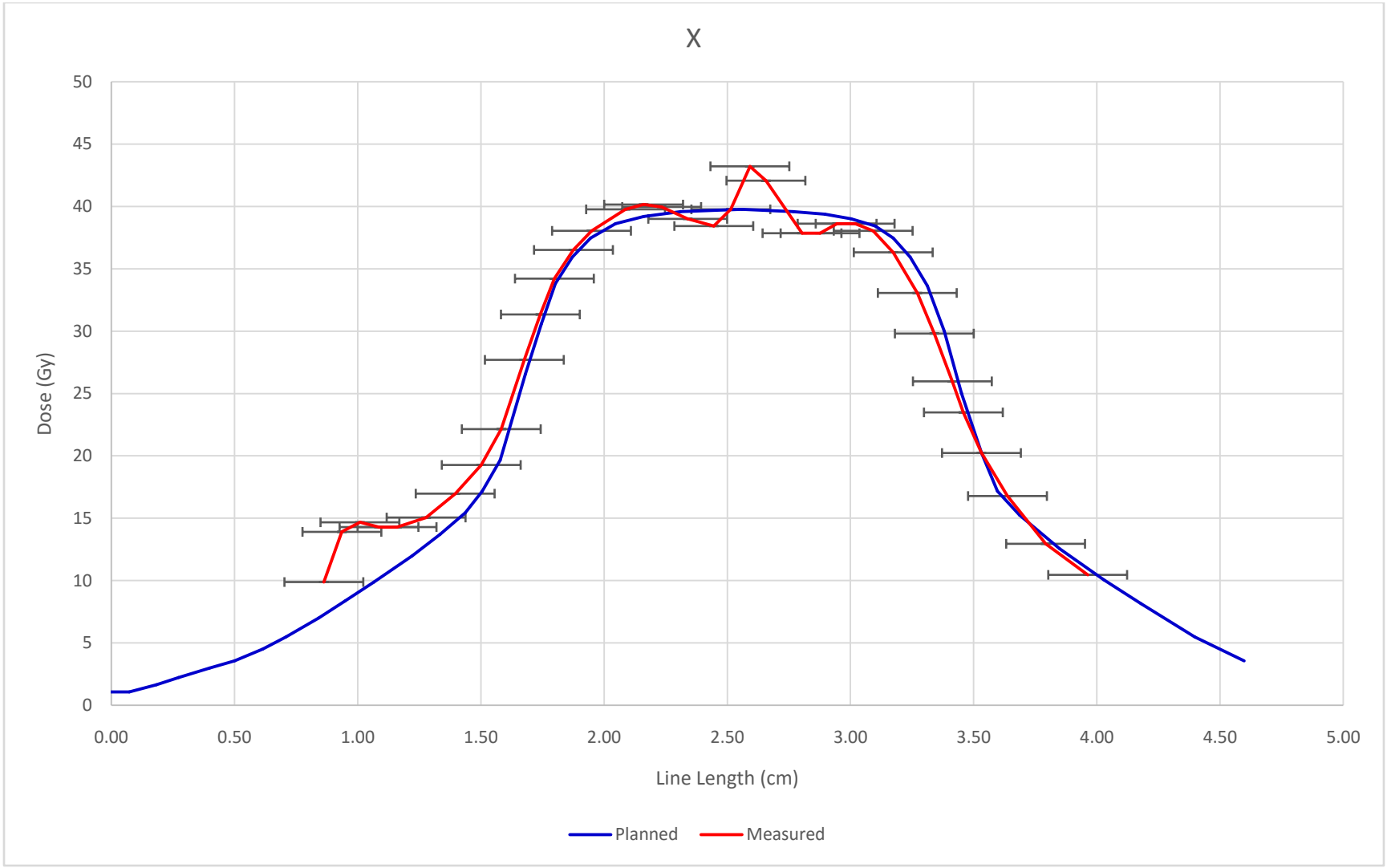

Figure 17: Evaluation 3 X-axis line-dose profile across sagittal plane

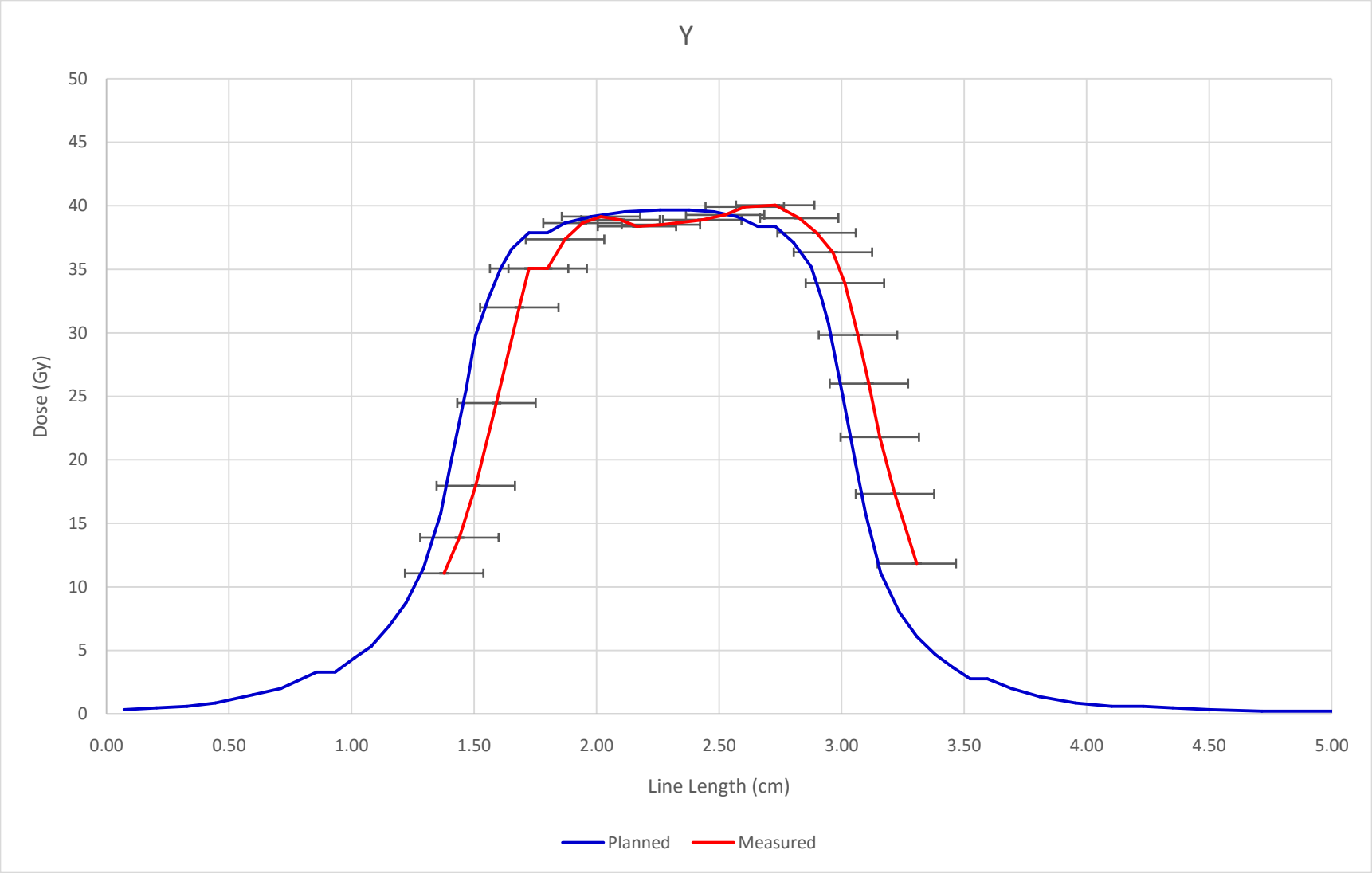

Figure 18: Evaluation 3 Y-axis line-dose profile across axial plane

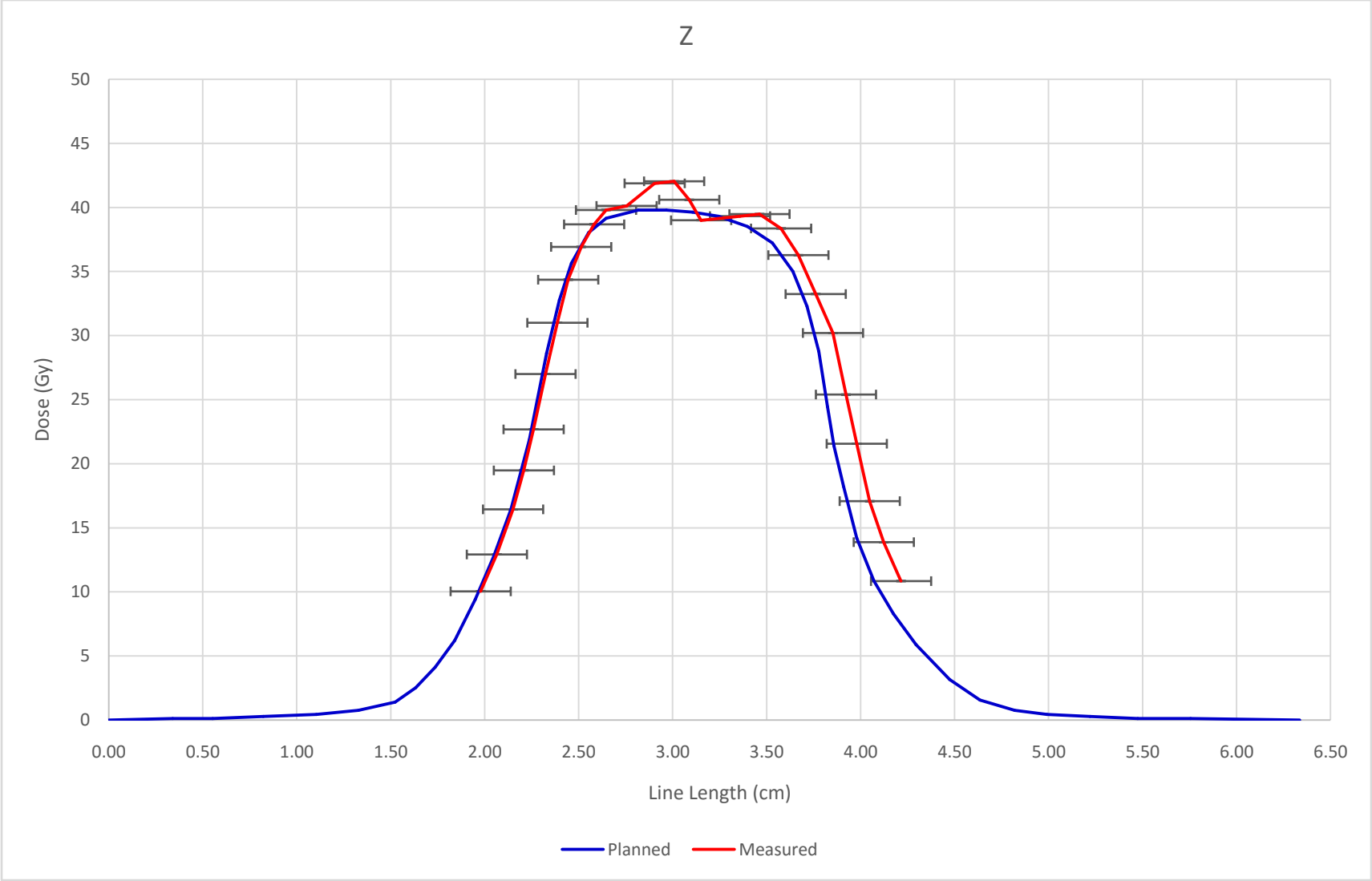

Figure 19: Evaluation 3 Z-axis line-dose profile across coronal plane

Figures 17 – 19 show the uncorrected data with uncertainty error bars for each line-dose profile. Each red line shows the measured results overlaid on top of the blue planned dose profile.For this evaluation, the uncertainty was determined to be 1.6 mm along the x-axis of each plot as determined earlier. Though this data does show that the measured dose distribution almost entirely fits within the acceptable range of error, the plots can be “corrected” by shifting the measured data sets within the acceptable range of uncertainty.This correction is not to minimize the visible shifts in data, but only to show the shapes of the spatial distributions in comparison to the planned profiles. The abscissa shifts can be seen in Figures 20 – 22 below.

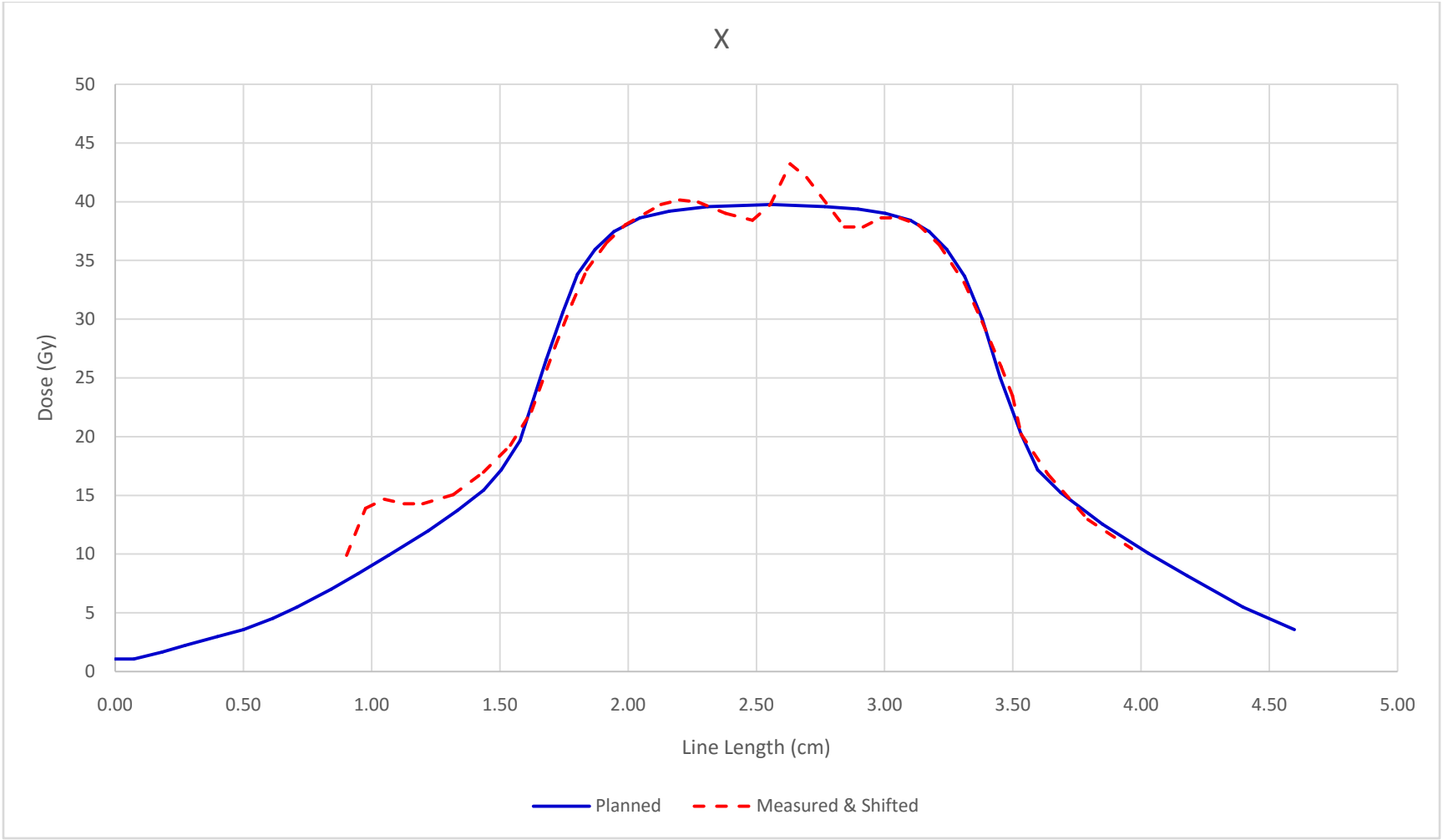

Figure 20: Evaluation 3 corrected X-axis line-dose profile across sagittal plane

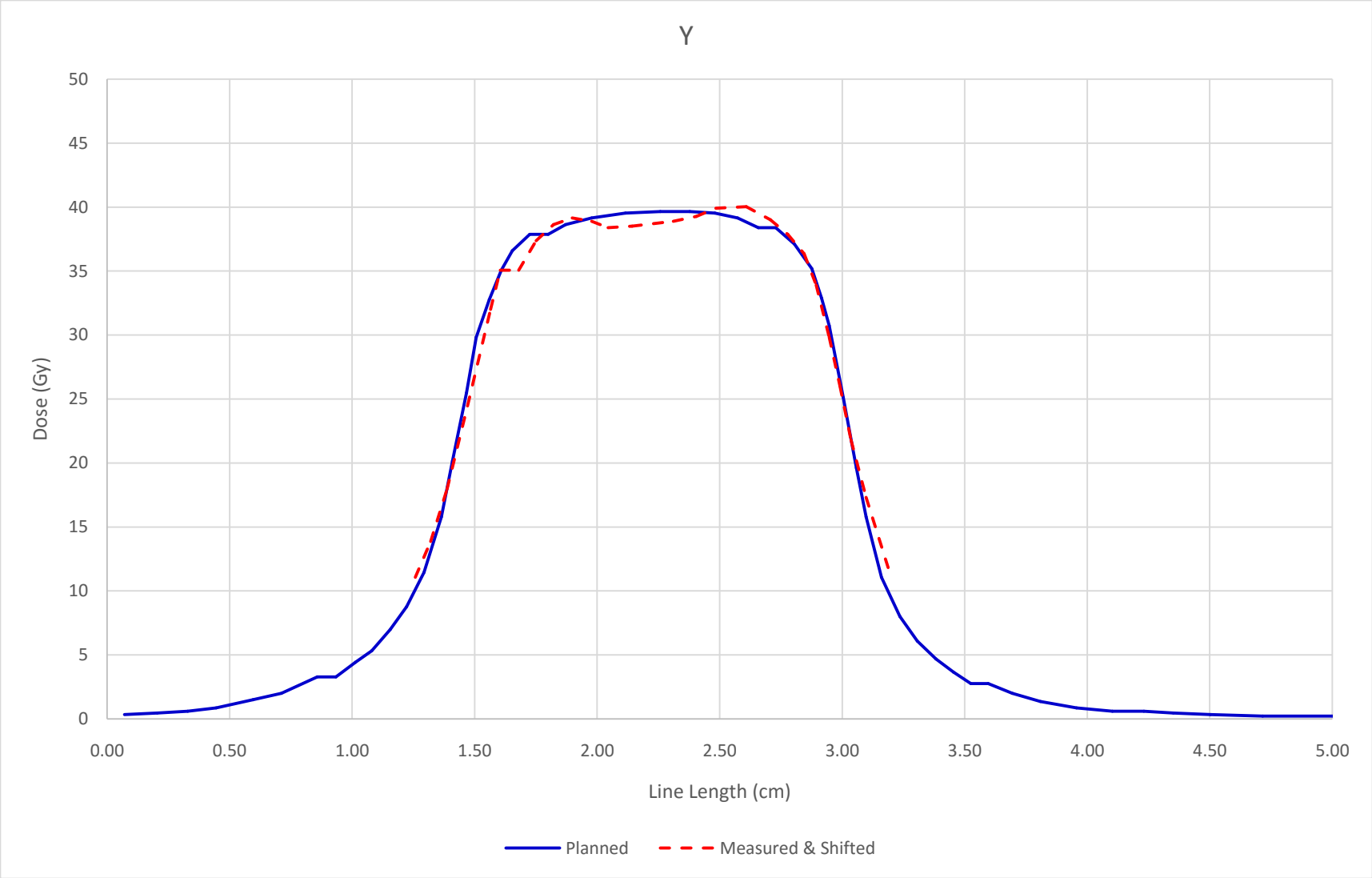

Figure 21: Evaluation 3 corrected Y-axis line-dose profile across axial plane

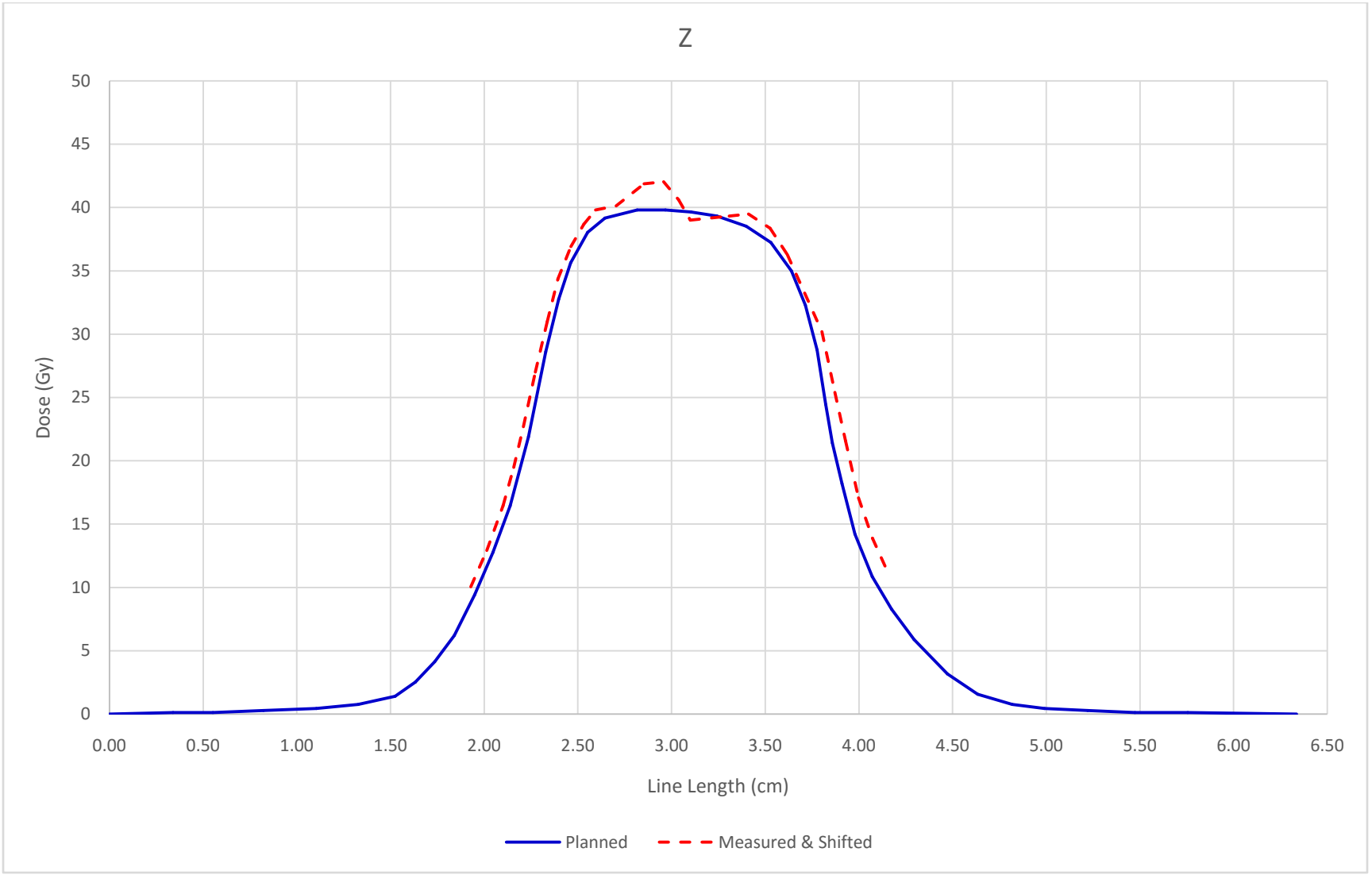

Figure 22: Evaluation 3 corrected Z-axis line-dose profile across coronal plane

These three plots may be more helpful in comparing the shape of the spatial distribution of the dose within the gel. Here, the X, Y, and Z axes were shifted by 0.40 mm, 1.2 mm, and -0.50 mm respectively. As noted earlier, the Y-axis seemed to show the largest shift in data between the planned and experimental distributions, which can be seen by the first set of line-dose profiles and the required shift in Figure 19. However, with the dotted red lines representing the data after a maximum of 1.2 mm in abscissa shift, the shape of each data set is clearly a match with the planned line-dose profile within the calculated limits of uncertainty.

4.0 DISCUSSION

4.1 Spatial Uncertainty

In this experiment, each evaluation's results fell within the calculated uncertainty for their respective procedure. The calculation of these uncertainties as discussed in Section 2.6 closely follow those of AAPM Task Group 42, who determined an achievable SRS accuracy of 2.4 mm in their report [6]. With a maximum individual uncertainty of 1.6 mm for each evaluation, the results of this evaluation fall well under acceptable limits for SRS.

For modern SRS treatments, similar calculations are used to determine the acceptable dose distribution based on three target volumes: gross tumor volume, clinical target volume, and planned target volume [35]. The gross tumor volume (GTV) is the extent of the tumor that can be imaged by conventional medical imaging techniques for treatment planning purposes. Surrounding the GTV is the clinical target volume (CTV), which not only includes the GTV, but also a localized region surrounding the GTV to account for the areas of the tumor that cannot be seen through imaging techniques.The volume encompassed in the CTV is typically a fixed value largely determined by the size of the GTV and the type of condition.

Lastly, surrounding both the GTV and the CTV is the planned target volume (PTV). This third volume accounts for uncertainties encountered during treatment delivery such as tissue movement, delivery tolerances of the equipment used to provide the treatment, and other geometric sources of uncertainty. In order for successful

treatment, this volume must be carefully contoured to encompass the entire tumor while avoiding other structures and healthy tissue that could be adversely affected by treatment.

For the acoustic neuroma condition simulated in this experiment, it is not uncommon for a 1-2 mm expansion of the PTV surrounding the tumor [36].Based on the acceptable amount of uncertainty calculated in this experiment, each test showed that the ClearView gel not only fell within these limits of geometric uncertainty, but also under the maximum amount typical of actual treatments for this condition. This compliance between both the experimental and clinical uncertainties shows promise that ClearView could be well suited for SRS commissioning and QA in terms of spatial resolution and geometric accuracy.

4.2Accelerator Dose Levels

Prior to the first dose delivery, the dose output accuracy of the TrueBeam accelerator was verified through several sequential measurements taken with an Exradin A16 ion chamber (Standard Imaging, Inc. - Middleton, WI) connected to a Capintec, Inc. (Ramsey, NJ) 192x Digital Dosimeter. From these measurements, the dose output of the accelerator was verified to have consecutive intensity measurements within 1% of each other.Throughout the course of the day, the readings are expected to remain within 2% of the morning test measurements. With the machine performing as expected, the dose discrepancy between the expected and measured data sets must lie somewhere within the procedure or the gel itself

As stated previously, the data used as a baseline for the scanner readings is a general calibration data set, which may vary from the accelerator used to irradiate the dosimeter.Gel batch variations also weigh heavily in the calibration data used to determine the dose received by the gel. Evaluation 3 showed much better response to the output of the TrueBeam system used in this experiment in comparison to both Evaluation 1 and 2, which showed to vary up to ten percent at the reported isocenter. The change between the third evaluation and the first two may be a result of batch variation during chemical gel production. Efforts to reduce batch variation are currently in effect at the Modus production facility.

Aside from the sources of uncertainty in the gel itself, other possible causes for the differences in reported dose levels are present. Differences in thickness and manufacturing of the vial containing the ClearView gelcan slightly affect the OD readings, which in turn could affect the measured dose level in the gel. Corrections for vial differences could be implemented once a baseline has been established for the CT scanner.The scanner can also have its output readings affected by the angle of the incident light to the curved surface of the vial, causing additional scatter in the OD measurement process. Again, corrections for these sources of uncertainty are currently being explored by the manufacturer.

4.3Future Work

Though ClearView gel shows promise of use in SRS commissioning and QA, further tests could explore other aspects of the gel to ensure that is a suitable replacement for current methods. Experiments across a wider range of dose delivery techniques could

show if the gel experiences limitations for SRS QA testing. Although all the tests in this experiment were performed at the same beam energy for consistency between evaluations, testing across a wider range of beam energies and dose rates could demonstrate how the gel reacts in terms of possible energy or dose rate dependence typical of other dosimetry techniques. In addition, tests across various temperatures could determine if temperature during irradiation has any significant effects on the measured output of the gel.

One alternative to relying solely on the ClearView gel dosimeter for not only spatial distribution but also absolute dose levels received by the gel is to use ClearView in addition to an output verification device. In this experiment, an Exradin A16 ion chamber was used prior to gel irradiation to determine the accuracy of the TrueBeam's output. Though the ion chamber is poorly suited for SRS dosimetry, the information obtained from preliminary measurements with an ion chamber could be used to normalize the dose distribution curve to match the output of the delivery system. Though the ClearView gel would not be the sole instrument required for SRS commissioning and QA, it could serve as an integral part of the QA process as a whole. Further testing could demonstrate the feasibility and effectiveness of this dual-instrumentation approach.

5.0 CONCLUSION

In this experiment, new ClearView gel dosimeterswere utilized to measure the output accuracy of a Varian TrueBeam particle accelerator. To test the dosimeter, three different evaluationswere performed that encompassed several factors of SRS: one static beam delivery, one full rotational arc about the central axis, and one full end-to-end SRS treatment plan simulating the treatment of an acoustic neuroma. The capabilities of the VistaView softwareallowed for direct comparison of the measured results obtained from the ClearView gel to the original treatment plans.

Based on the composed line-dose profiles for each of the three evaluations, it wasverified that the tetrazolium salt-based ClearView gel dosimeter was geometrically accurate within the calculated window of uncertainty for every evaluation performed in this project.The sub-millimeter accuracy of the ClearView gel allows precise determination of the target isocenter after irradiation as well as how much additional dose is delivered to the surrounding tissue within the steep dose gradients. Though ClearView shows promise for SRS commissioning and QA due to its high spatial dose distribution in three dimensions, further testing of reported dose would be needed to verify its use as a standalone dosimeter for small field dosimetry.

The capability to determine accurately measure spatial dose distribution for these small-field dose geometries suggests that ClearView could be applied to other treatment methods employing small-field dosimetry QA. Small-field volumetric modulated arc therapy (VMAT) and intensity modulated radiation therapy (IMRT) could be appropriate uses of ClearView gel to determine accuracy during commissioning and QA.

REFERENCES

1. Pike, B. et al. “Dose distributions in dynamic stereotactic radiosurgery.” *Medical Physics* 14(5), 1987, pp 780-789

2. Podgorsak, E. B. et al. “Dynamic stereotactic radiosurgery.” *International Journal of Radiation Oncology, Biology, Physics* 14(1), 1987, pp 115-126

3. Nieder, C., Grosu, A., and Gaspar, L. “Stereotactic radiosurgery (SRS) for brain metastases: a systematic review.” *Radiation Oncology* 9(155), 2014, pp 1-9

4. Das, I. et al. “Choice of radiation detector in dosimetry of stereotactic radiosurgery-radiotherapy.” *Journal of Radiosurgery* 3(4), 2000, pp 177-186

5. Drzymala, R, et al. “Assurance of high quality LINAC-BASED stereotactic radiosurgery.” *International Journal of Radiation Oncology, Biology, Physics* 30(2), 1994, pp 459-472

6. Schell, M. C. et al. “Stereotactic Radiosurgery: AAPM Report 54 of Task Group 42.” *American Association of Physicists in Medicine,*Report 54. College Park, MD, 1995

7. Soldberg, T. et al. “Quality and safety considerations in stereotactic radiosurgery and stereotactic body radiation therapy: Executive summary.” *Practical Radiation Oncology* 2, 2012, pp 2-9

8. Heydarian, M., Hoban, P., and Beddoe, A. “A comparison of dosimetry techniques in stereotactic radiosurgery.” *Physics in Medicine and Biology* 41(1), 1996, pp 93-110

9. Novotny, J. Jr. et al. “Quality control of the stereotactic radiosurgery procedure with the polymer-gel dosimetry.” *Radiotherapy and Oncology* 6, 2002, pp 223-230

10. Pappas, E. et al. “Small SRS photon field profile dosimetry performed using a PinPoint air ion chamber, a diamond detector, a novel silicon-diode array (DOSI), and polymer gel dosimetry. Analysis and intercomparison.” *Medical Physics* 35(10), 2008, pp 4640-4648

11. Novotny, J. et al. “Quality control of the stereotactic radiosurgery procedure with polymer gel dosimetry.” *Radiotherapy and Oncology* 63, 2002, pp 223-230

12. Appleby, A. and Leghrouz, A.“Imaging of radiation dose by visible color development in ferrous agarose xylenol-orange gels.”*Medical Physics* 18, 1991,pp 309-312

13. Godson, H. et al. “Analysis of small field percent depth dose and profiles: Comparison of measurements with various detectors and effects of detector orientation with different jaw settings.” *Journal of Medical Physics* 41(1), 2016, pp 12-20

14. Duggan, D. and Coffey, C. “Small photon field dosimetry for stereotactic radiosurgery.” *Medical Dosimetry* 23(3), 1998, pp 153-159

15. Taylor, M., Kron, K., and Franich, R. “A contemporary review of stereotactic radiotherapy: Inherent dosimetric complexities and the potential for detriment.” *Acta Oncologica* 50, 2011, pp 483-508

16. Bucciolini, M. et al. “Diamond detector versus silicon diode and ion chamber in photon beams of different energy and field size.” *Medical Physics* 30(8), 2003, pp 2149-2154

17. Esparza-Moreno, K. et al. “Comparison of trigeminal neuralgia radiosurgery plans using two film detectors for the commissioning of small photon beams.” *Journal of Applied Clinical Medical Physics* 14(6), 2013, pp 18-26

18. Ertl, A. et al. “TLD array for precise dose measurements in stereotactic radiation techniques.” *Physics in Medicine and Biology* 41, 1996, pp 2679-2686

19. Avila-Rodriguez, M., Rodririguez-Villafuerte, M., and Perches, R. “Stereotactic radiosurgery dosimetry using thermoluminescent dosimeters and radiochromic films.” *American Institute of Physics Conference Proceedings* 538(1), 2000, pp 213-218

20. Baldock, C. et al. “Topical Review: Polymer gel dosimetry.” *Physics in Medicine and Biology* 55(5), 2010, pp R1-R63

21. Guo, P., Adamovics, J, and Oldham, M. “A practical three-dimensional dosimetry system for radiation therapy.” *Medical Physics* 33(10), 2006, pp 3962-3972

22. Fricke, H. and Morse, S. “The chemical action of roentgen rays on dilute ferrous sulphate solutions as a measure of radiation dose.” *American Journal Roentgenology, Radium Therapy and Nuclear Medicine* 18, 1927, pp 430-432

23. Gore, J. C., Yang, Y. S., and Schulz, R. I. “Measurement of radiation dose distributions by nuclear magnetic resonance (NMR) imaging.”*Physics in Medicine and Biology*29, 1984,pp 1189-1197

24. Schreiner, L. J. “Review of Fricke gel dosimeters.” *Journal of Physics: Conference Series* 3, 2004, pp 9-21

25. Hazle, J. D. et al. “Dose-response characteristics of a ferrous-sulphate-doped gelatin system for determining radiation adsorbed dose distributions by magnetic resonance imaging (Fe MRI).” *Physics in Medicine and Biology*36(8), 1991, pp 1117-1125

26. Appleby, A., Christman, E. A., and Leghrouz, A. “Imaging of spatial radiation dose distribution in agarose gels using magnetic resonance.” *Medical Physics* 14(3), 1987, pp 382-384

27. Appleby, A. and Leghrouz, A. “Imaging of radiation dose by visible color development in ferrous-agarose-xylenol orange gels.” *Medical Physics* 18(2), 1991, pp 309-312

28. Olsson, L. E. et al. “Ferrous sulphate gels for determination of absorbed dose distributions using MRI technique: basic studies.” *Physics in Medicine and Biology*34(1), 1989, pp 43-52

29. Baldock, C. “Historical overview of the development of gel dosimetry: a personal perspective.”*Institute of Physics Publishing. Journal of Physics: Conference Series* 56, 2006,pp 14-22

30. Alexander, P. et al. “The degredation of solid polymethylmethacrylate by ionizing radiations.” *Proceedings of the Royal Society A* 223(1154), 1954, pp 392-404

31. Cosgrove, V. et al. “The reproducibility of polyacrylamide gel dosimetry applied to stereotactic conformal radiotherapy.” *Physics in Medicine and Biology* 45, 2000, pp 1195-1210

32. Coffey, C. et al.“A tissue equivalent phantom for stereotactic radiosurgery localization and dose verification.”*Stereotactic Functional Neurosurgery* 61(S1),1993, pp 130-141.

33. Hong, R. S. and Kartush, J. M. “Acoustic neuroma neurophysiologic correlates: facial and recurrent laryngeal nerves before, during, and after surgery.”*Otolaryngologic Clinics of North America* 45(2), 2012, pp 291-306

34. Ramaseshan, R. and Heydarian, M. “Comprehensive quality assurance for stereotactic radiosurgery treatments.”*Physics in Medicine and Biology* 48(14), 2003, pp N199-N205

35. Burnet, N. et al. “Defining the tumour and target volumes for radiotherapy.” *Cancer Imaging* 4(2), 2004, pp 153-161

36. Koh, E. et al. “Fractionated stereotactic radiotherapry for acoustic neuroma.” *Cancer* 109(6), 2007, pp 1203-1210